Embargo by Cell press until 21.11.19

Microbiota-derived lactate activates production of reactive oxygen species by the intestinal NADPH oxidase Nox and shortens *Drosophila* lifespan

Igor Iatsenko[*], Jean-Philippe Boquete, Bruno Lemaitre[*#]

Global Health Institute, School of Life Sciences, Ecole Polytechnique Fédérale de Lausanne (EPFL), Station 19, 1015 Lausanne, Switzerland

*Corresponding author:

I.I.: igor.iatsenko@epfl.ch

B.L.: bruno.lemaitre@epfl.ch

#Lead contact: B. L.: bruno.lemaitre@epfl.ch

Summary

Commensal microbes colonize the gut epithelia of virtually all animals and provide several benefits to their hosts. Changes in commensal populations can lead to dysbiosis, which is associated with numerous pathologies and decreased lifespan. Peptidoglycan recognition proteins (PGRP) are important regulators of the commensal microbiota and intestinal homeostasis. Here, we found that a null mutation in *Drosophila PGRP-SD* was associated with overgrowth of *Lactobacillus plantarum* in the fly gut and a shortened lifespan. *L. plantarum*-derived lactic acid triggered the activation of the intestinal NADPH oxidase Nox and the generation of reactive oxygen species (ROS). In turn, ROS production promoted intestinal damage, increased proliferation of intestinal stem cells and dysplasia. Nox-mediated ROS production required lactate oxidation by the host intestinal lactate dehydrogenase, revealing a host-commensal metabolic crosstalk that is likely broadly conserved. Our findings outline a mechanism whereby host immune dysfunction leads to commensal dysbiosis that in turn promotes age-related pathologies.

Introduction

The epithelial surfaces of most metazoan organisms are inhabited by complex microbial communities (Hooper and Gordon, 2001). The composition of these microbial communities is determined by an intricate interplay of genetic and environmental factors (Ley et al., 2006). Changes in healthy microbiota composition, referred to as commensal dysbiosis, have been associated with pathologies like inflammatory bowel disease, obesity, diabetes, neurological disorders, chronic inflammation and cancer (Clemente et al., 2012; Garrett et al., 2010). However, the vast diversity of mammalian microbiota and genetic complexity of the immune system are major obstacles to clearly establishing mechanistic links between host immune genotype, microbiota structure and disease phenotype.

Because of the simplicity of its microbiota and physiological similarity with the mammalian intestine, the *Drosophila* gut is a model of choice to study human intestinal pathophysiology (Apidianakis and Rahme, 2011; Liu et al., 2017). Studies using this model have provided insights into innate immunity signaling, host-commensal interactions, and epithelial homeostasis during aging (Bae et al., 2010; Biteau et al., 2011; Broderick et al., 2014; Buchon et al., 2009a, 2009b, 2013; Capo et al., 2016; Lemaitre and Hoffmann, 2007; Martino et al., 2017). *Drosophila* harbors a microbiota composed of 5 to 30 bacterial species, dominated by the genera *Acetobacter* and *Lactobacillus* (Broderick and Lemaitre, 2012; Wong et al., 2013, 2011). Although many *Drosophila* commensals inhabit the gut transiently and are constantly replenished from food, they affect various aspects of host physiology ranging from the promotion of larval growth to the defense against pathogens (Blum et al., 2013; Broderick et al., 2014; Martino et al., 2017; Pais et al., 2018; Sannino et al., 2018; Sharon et al., 2010; Storelli et al., 2011, 2018). As in humans, dysbiosis in flies is associated with disruption of gut homeostasis, inflammation and reduced lifespan, highlighting the importance of maintaining healthy microbiota composition and abundance (Clark et al., 2015; Guo et al., 2014; Li et al., 2016; Ryu et al., 2008; Sekihara et al., 2016).

Several host mechanisms restrict growth of both symbiotic and pathogenic bacteria in the *Drosophila* gut. Acid secretion by V-ATPases of the copper cell region in the middle midgut has been shown to eliminate most intestinal bacteria (Li et al., 2016; Overend et al., 2016; Storelli et al., 2018), while a chitinous barrier, the peritrophic matrix, shields epithelial cells from invading bacteria (Kuraishi et al., 2011). Moreover, two inducible host defense mechanisms control both pathogens and microbiota in the gut: antimicrobial peptides (AMPs) and reactive oxygen species (ROS) (Buchon et al., 2009a; Ha et al., 2005; Ryu et al., 2006; Tzou et al., 2000). Two ROS producing enzymes, the NADPH oxidases Duox and Nox, have been implicated in the control of intestinal microbes in *Drosophila*. The dual oxidase Duox (Ha et al., 2005) produces microbicidal ROS in response to uracil released by pathogenic bacteria (Lee et al., 2013). Nox produces ROS in response to commensal bacteria, such as *L. plantarum*, but how Nox is activated is not yet

known (Jones et al., 2013). ROS not only eliminate ingested pathogens but also damage enterocytes, thereby promoting the compensatory proliferation of intestinal stem cells (Buchon et al., 2009b; Hochmuth et al., 2011).

In addition to triggering ROS, ingested bacteria activate the expression of several antimicrobial peptide genes in specific domains along the digestive tract (Buchon et al., 2009a; Tzou et al., 2000; Zhai et al., 2018). This response is initiated when DAP-type peptidoglycan from Gram-negative bacteria is sensed by the transmembrane recognition receptor PGRP-LC in the ectodermal parts of the gut or by the intracellular receptor PGRP-LE in the midgut (Bosco-Drayon et al., 2012; Buchon et al., 2009a; Kaneko et al., 2004; Kleino and Silverman, 2014; Neyen et al., 2012). PGRP-LC and PGRP-LE then recruit the adaptor IMD to finally activate the NF-κB-like transcription factor Relish (Kleino et al., 2017). The gut antibacterial response is kept in check by several negative regulators of the IMD pathway, notably by enzymatic PGRPs such as PGRP-LB and PGRP-SC that scavenge peptidoglycan. Flies lacking these negative regulators show excessive, deleterious local and systemic immune activation (Aggarwal et al., 2008; Charroux et al., 2018; Kleino et al., 2008; Lhocine et al., 2008; Paredes et al., 2011; Zaidman-Rémy et al., 2006).

The IMD pathway also shapes the commensal community structure in the intestine. For example, *PGRP-LC* and *relish* flies with defects in the IMD pathway are short-lived and exhibit increased bacterial loads in their guts upon aging (Buchon et al., 2009b). Chronic over-activation of the IMD pathway is also associated with microbiota dysbiosis, characterized by the expansion of antimicrobial peptide-resistant pathobionts (Ryu et al., 2008). However, the mechanism whereby immune dysfunction causes commensal dysbiosis and leads to age-related pathologies and lifespan reduction is not fully understood.

We previously identified *Drosophila* PGRP-SD as a secreted pattern recognition receptor which functions upstream of PGRP-LC to enhance IMD pathway activation during systemic infection (Iatsenko et al., 2016; Monahan et al., 2016). In contrast to canonical mutants of the IMD pathway, a null mutation in *PGRP-SD* reduces but does not abolish the immune response, providing a sensitive tool to study the IMD pathway. In this study, we used the sensitized *PGRP-SD* background to investigate the role of IMD pathway in the control of intestinal homeostasis during infection and aging. Specifically, we asked whether PGRP-SD was required to maintain a stable commensal composition, and whether loss of PGRP-SD would lead to intestinal dysbiosis and dysplasia.

Results

PGRP-SD is induced by oral infection in an IMD-dependent manner

To study the role of *PGRP-SD* in the gut immune response, we monitored its expression profile in the gut by RT-qPCR after *Erwinia carotovora* (*Ecc15*) and *Pseudomonas entomophila* (*Pe*) oral infections (Basset et al., 2000; Vodovar et al., 2005). *PGRP-SD* was induced at 6h and 24h post infection in wild-type but not in *Relish* or *PGRP-LE* mutant guts (Figure 1A, Figure S1A), indicating that *PGRP-SD* expression in the gut is under IMD pathway control. To visualize the expression pattern of *PGRP-SD* in the gut, we generated a *PGRP-SD-GAL4* line in which the GAL4 gene is under the control of 177 bp of *PGRP-SD* upstream sequence (Figure 1B). The cloned region contains two canonical conserved Relish-binding sites (Figure 1B), consistent with the fact

that PGRP-SD expression is under control of Relish (Buchon et al., 2009a). *PGRP-SD-GAL4;UAS-mCD8::GFP* expression was not detected in uninfected flies. However, *Ecc15* infection induced GFP expression in the proventriculus, the copper cell region, and in small cells scattered over the entire gut (Figure 1C, Figure S1B). These cells were negative for the enteroendocrine cell marker Prospero, indicating that they are not enteroendocrine cells but rather progenitor cells (Figure S1B'). Most of them were positive for the intestinal stem cells marker Delta, suggesting that largely these cells represent intestinal stem cells (Figure S1B"). This expression pattern corresponds to regions already reported to be IMD pathway responsive (Fink et al., 2016). Thus, PGRP-SD is a bona-fide IMD pathway gene that responds to bacterial stimulus in the gut.

PGRP-SD is required in the gut for IMD pathway activation and defense against oral infections

To further analyze the role of PGRP-SD in the intestinal immune response, we used *PGRP-SD^{sk1}* mutants that we previously generated using CRISPR-Cas9 method. The *PGRP-SD^{sk1}* allele has a small deletion, which induces a frameshift causing a premature stop codon and leading to a peptide of 50 residues lacking the PGRP domain (Iatsenko et al., 2016). We measured the expression of *Diptericin* (*Dpt),* a readout of the IMD pathway, by RT-qPCR in the guts of *PGRP-SD^{sk1}* mutants after *Ecc15* and *Pe* oral infections. *Dpt* was significantly lower in the mutant compared to wild-type flies 6h and 24h post-infection (Figure 1D, Figure S1C). In line with these results, *PGRP-SD^{sk1}* mutants carrying a *Dpt-lacZ* reporter showed weaker gut X-gal staining after *Ecc15* oral infection compared to wild-type flies (Figure S1D-E). RNAi-mediated silencing of *PGRP-SD* using specific GAL4 drivers in *PGRP-SD*-positive cells (*pPGRP-SD-GAL4*), in midgut enterocytes (*Myo1A-GAL4*), in copper cells (*Labial-GAL4*), and in stem cells (*esg-GAL4*) mimicked the *PGRP-SD^{sk1}* mutant phenotype upon *Ecc15* oral infection (Figure 1E). Ubiquitous (*Act-GAL4*), gut-specific (*Myo1A-GAL4*), and *PGRP-SD*-cell specific overexpression of *PGRP-SD* was sufficient to restore the expression of *Dpt* in the mutant after *Ecc15* infection (Figure 1F). Consistent with reduced IMD pathway activation, *PGRP-SD^{sk1}* homozygous and transheterozygous mutants (Figure 1G), and *PGRP-SD* RNAi flies (Figure S1F) showed increased sensitivity to *Pe* oral infection. Altogether, our data show that PGRP-SD plays a role in the gut by promoting IMD pathway activation, akin to its role in the systemic immune response.

PGRP-SD is necessary for microbiota-induced expression of negative regulators in the gut

Considering that a null mutation in *PGRP-SD* reduces but does not completely block the immune response, the *PGRP-SD^{sk1}* mutant provides a sensitive tool to probe the role of the IMD pathway in the control of microbiota. We found higher *PGRP-SD* expression in the guts of conventionally raised flies (with their endogenous microbiota) compared to their axenic counterparts (Figure 1H). Similarly, intestinal *PGRP-SD* expression increased when axenic wild-type flies were fed *L. plantarum (Lp^{WJL}),* a representative member of the microbiota. This induction was completely blocked in *PGRP-LE* but not in *PGRP-LC* mutants, indicating that *PGRP-SD* is induced by the microbiota in a PGRP-LE-dependent manner in the midgut (Figure 1I). We next investigated whether PGRP-SD modulates IMD pathway activity to commensal bacteria. To achieve this in a controlled way, axenic flies were recolonized with a defined quantity of *Lp^{WJL}* (see methods) and tested for IMD pathway activation 6h after. Contrasting with *Ecc15* infection, oral ingestion of the symbiotic bacterium *Lp^{WJL}* induced a low level of *Dpt* expression (Figure 1J) but a high level of *PGRP-SD*-dependent expression of *PGRP-LB*, *PGRP-SC1*, and *pirk* that encode negative

regulators (Figure 1K, Figure S1G-H). The fact that a commensal bacterium strongly induces expression of negative regulators likely contributes to the immune tolerance to colonizing bacteria.

Previous studies have shown that *PGRP-LB* mutant flies have higher systemic immune activation upon oral infection due to the transfer of uncleaved PGN from the gut lumen to the hemolymph (Zaidman-Rémy et al., 2006). Given that PGRP-SD is required in the gut for the expression of negative regulators of the IMD pathway, *PGRP-SD^{sk1}* mutants might also show a higher systemic immune activation upon oral infection. We were indeed able to detect a much stronger systemic *Dpt* expression in *PGRP-SD^{sk1}* mutant flies compared to wild-type at 24h and 48h post *Ecc15* oral infection (Figure S1J). Importantly, overexpression of *PGRP-SD* or *PGRP-LB* in enterocytes was sufficient to restore systemic *Dpt* expression to wild-type levels in *Ecc15*-infected *PGRP-SD* mutants (Figure S1J). These results indicate that PGRP-SD, by controlling the expression of negative regulators of the IMD pathway in the gut, also contributes to immune tolerance to commensal bacteria.

PGRP-SD^{sk1} mutants show reduced lifespan and age-related dysplasia

Alterations of the IMD pathway have been associated with reduced lifespan (Capo et al., 2016; Liu et al., 2017). This together with the fact that *PGRP-SD* expression increases with age (Figure S2A, Guo et al., 2014) prompted us to assess the lifespan of *PGRP-SD^{sk1}* mutants. Conventionally reared *PGRP-SD^{sk1}* flies live significantly shorter compared to wild-type flies (Figure 2A). Eliminating the microbiota by putting flies on antibiotics-supplemented food strongly increases the lifespan of *PGRP-SD^{sk1}* mutants, indicating that the microbiota contributes to the premature death of the mutant. One of the aging hallmarks in flies is intestinal stem cell (ISCs) over-proliferation and mis-differentiation leading to dysplasia (Biteau et al., 2010, 2011; Choi et al., 2008; Guo et al., 2014; Li et al., 2016). Use of an intestinal progenitor marker (*esg-GAL4, UAS-GFP)* confirmed that young wild-type flies (3d old) had a low level of epithelium renewal, which strongly increased in 21d old flies (Figure 2B). ISCs proliferation in 21d old *PGRP-SD^{sk1}* mutant was much higher compared to wild-type flies. This phenotype was dependent on the microbiota since under axenic conditions ISCs overproliferation in the mutant was rescued (Figure 2B). Consistent with this, immunostainings with an antibody against Phospho-Histone 3 (PH3), a specific marker for mitotic cells, revealed more PH3 positive cells in 21d old conventional but not axenic *PGRP-SD^{sk1}* mutant flies compared to wild type (Figure 2C). These results indicate that *PGRP-SD^{sk1}* mutants are short-lived likely due to microbiota-driven dysplasia.

To confirm that the observed lifespan and dysplasia phenotypes are indeed due to the mutation in *PGRP-SD*, we performed a rescue experiment, where we overexpressed *PGRP-SD* with the *pPGRP-SD-GAL4* driver. This was sufficient to partially rescue the lifespan and PH3 counts in *PGRP-SD^{sk1}* mutants (Figure S2B-C).

Previous studies have shown that the JAK-STAT pathway regulates the level of epithelial renewal by stimulating ISCs proliferation (Buchon et al., 2009b; Jiang et al., 2009). We observed that JAK-STAT pathway ligands of the Unpaired family (Upds) were expressed at higher levels in 21d old *PGRP-SD^{sk1}* mutant guts compared to wild-type guts (Figure 2D, S2D). We obtained similar results using a reporter line of JAK-STAT pathway activation (10×Stat-GFP) (Figure S2E). In contrast, both wild-type and *PGRP-SD^{sk1}* mutant flies had low mitotic counts and reduced JAK-STAT pathway activity under axenic conditions (Figure 2D, S2D). In line with this, blocking the JAK-STAT pathway by gut-specific RNAi-mediated silencing of *upd2* elongated lifespan (Figure 2E) and prevented ISC over-proliferation in the *PGRP-SD^{sk1}* mutant (not shown). Thus, the IMD

pathway regulator PGRP-SD contributes to intestinal homeostasis by preventing microbiota-driven intestinal dysplasia.

Overgrowth of *Lp* shortens lifespan of *PGRP-SD^{sk1}* mutants

Considering that commensal dysbiosis is frequently associated with age-related host mortality (Buchon et al., 2009b; Guo et al., 2014), we assessed diversity and abundance of microbiota in wild-type and *PGRP-SD^{sk1}* mutant flies. To do this, we generated 16S rRNA clone libraries from DNA extracted from whole 21 day old wild-type and *PGRP-SD^{sk1}* mutant flies. As shown in Figures 3A and S3A, the vast majority (>95%) of microbes matched *Lp* irrespective of the host genetic background and fly age. Rare clones were identified as *Acetobacter pomorum, A. pasteurianus, Enterococcus sp., Gluconobacter sp., L. brevis,* which are frequently found in the *Drosophila* gut (Wong et al., 2013). With this approach, we found that both wild type and *PGRP-SD* mutant flies are predominantly colonized with *L. plantarum*, suggesting that their differences in the lifespan are unlikely due to changes in microbiota composition. Therefore, next we checked the abundance of the microbiota in wild type and mutant flies by plating whole fly homogenates on MRS agar plates. We consistently recovered nearly 10 times more bacteria from *PGRP-SD^{sk1}* mutants compared to wild-type flies (Figure 3B). Using qPCR with bacteria-specific primers, we confirmed that *PGRP-SD^{sk1}* mutants harbor more *Lp* than wild-type flies, while *Acetobacter* in the same samples was barely detected (Figure 3C, S3B). Therefore, we reasoned that differences in the lifespan between *PGRP-SD^{sk1}* and wild-type flies were unlikely due to changes in microbiota composition but rather due to overgrowth of *Lp*. To test this hypothesis, we colonized axenic wild-type and *PGRP-SD^{sk1}* mutant flies with a *Lp* strain (*Lp^{SD}*) isolated from the *PGRP-SD^{sk1}* mutant. These *Lp^{SD}*-mono-associated 21d old *PGRP-SD^{sk1}* mutant flies showed higher expression of the JAK-STAT pathway ligand *upd3* compared to wild-type flies, which is indicative of stronger JAK-STAT pathway activation (Figure 3D). Similarly, we detected significantly more PH3 positive cells in the guts of *PGRP-SD^{sk1}* mutant flies colonized with *Lp^{SD},* which is a sign of increased ISC proliferation and dysplasia (Figure 3E). Also, the lifespan of *PGRP-SD^{sk1}* mutant flies colonized with *Lp^{SD}* was substantially reduced compared to wild-type flies (Figure 3F). Thus, the colonization of axenic flies with *Lp* fully recapitulates phenotypes of conventional flies, indicating that the overgrowth of this microbe is the major cause of reduced lifespan in the *PGRP-SD^{sk1}* mutant. Finally, we found that the lifespan of *PGRP-SD^{sk1}* mutant flies colonized with a wild type microbiota is similarly reduced as in *PGRP-SD^{sk1}* mutant flies colonized with their native microbiota. Also, the lifespan of wild-type flies was not affected by *PGRP-SD^{sk1}* microbiota. These microbiota transplantation experiments (Figure 3G) further proved that lifespan differences unlikely stem from changes in microbiota composition but rather from overproliferation of *Lp* in *PGRP-SD^{sk1}* mutant flies. We next investigated if other microbiota member could induce similar phenotypes as *Lp* in *PGRP-SD^{sk1}* mutants. Colonization of axenic flies with *A. pomorum* (*Ap*) also resulted in lifespan reduction and ISC proliferation (Figure S3C, S3D). However, this effect was not as dramatic as in case of *Lp*, and *Ap* affected both wild-type and *PGRP-SD^{sk1}* flies to the same degree. Also, there was not over-growth of *Ap* in *PGRP-SD^{sk1}* mutants (Figure S3E), indicating that not every microbiota member is excessively detrimental to *PGRP-SD^{sk1}* mutant.

In addition, we observed that disruption of IMD pathway in another mutant, *Relish*, also results in overgrowth of *Lp* similar to *PGRP-SD^{sk1}* mutants. Also, *Relish* mutants have reduced lifespan and increased ISC proliferation (Figure S3F-H), suggesting that IMD pathway in general is a crucial regulator of intestinal homeostasis.

Induction of ROS by Nox but not Duox triggers dysplasia in *PGRP-SD^{sk1}* mutants

In the *Drosophila* gut, oxidative stress has been shown to be both necessary and sufficient to trigger intestinal stem cell proliferation (Biteau et al., 2011; Hochmuth et al., 2011; Xu et al., 2017). This prompted us to explore the role of ROS in the age-related dysplasia of *PGRP-SD^{sk1}* flies. We detected a higher amount of ROS in 21d old *PGRP-SD^{sk1}* mutant compared to wild-type guts, using both Dihydroethidium (DHE) staining (Figure S4A) and fluorometric ROS detection (Figure 4A). The level of ROS was significantly ($p \leq 0.05$) lower in axenic flies with no difference between wild-type and *PGRP-SD^{sk1}* mutant (Figure 4A, S4A). Re-association of axenic flies with *Lp^{SD}* was sufficient to induce ROS accumulation in fly guts (Figure 4B), suggesting that *Lp* specifically is responsible for ROS induction.

When we fed flies with the antioxidant N-acetyl cysteine (NAC), it was sufficient to reduce the amount of ROS in *PGRP-SD^{sk1}* mutant guts to wild-type level (Figure S4B). Antioxidant food also decreased the level of ISC proliferation (PH3 counts) and JAK-STAT pathway activity as measured by *upd3* expression in the mutant (Figure S4C, Figure 4C). Also, *PGRP-SD^{sk1}* mutants maintained on NAC-supplemented food lived longer compared to flies on standard food (Figure 4D), suggesting that ROS contribute at least partially to the mutant's early mortality.

In *Drosophila*, Nox and Duox enzymes have been implicated before in ROS production in response to bacteria. Thus, we next investigated the source of ROS by RNAi-mediated silencing of *Nox* and *Duox* in flies mono-associated with *Lp^{SD}*. We observed that *Lp^{SD}* triggered ROS in control and *Duox RNAi* flies, but not in *Nox RNAi* flies (Figure 4E). In addition, *Nox* but not *Duox RNAi* significantly suppressed ROS generation in the *PGRP-SD^{sk1}* mutant (Figure 4E). Consistent with this, *Nox* inhibition by RNAi partially decreased the levels of JAK-STAT pathway activity (*upd3* expression) and stem cell proliferation (PH3 counts) in the mutant (Figure 4F, 4G). Furthermore, the lifespan of the *PGRP-SD^{sk1}* mutant was significantly prolonged when *Nox* was inhibited by RNAi (Figure 4H). Therefore, all aging-related hallmarks of *PGRP-SD^{sk1}* mutant flies can be at least partially rescued by Nox inhibition.

Lp overgrowth acidifies the intestine of *PGRP-SD^{sk1}* mutant flies

Pathogen-derived uracil induces Duox-dependent ROS production (Lee et al., 2013), but how Nox-dependent ROS production is activated is unclear. *Lp* is a representative of Lactic Acid Bacteria (LAB), which frequently acidify substrates due to the release of large amounts of lactic acid (Pfeiler and Klaenhammer, 2007). This raises the possibility that ROS production is a secondary consequence of acid production. We first assessed the gut pH of wild-type and *PGRP-SD^{sk1}* mutants by feeding flies with the pH-sensitive dye bromophenol blue. As previously shown (Li et al., 2016; Overend et al., 2016), young wild-type flies (5d old) have an acidic region in the central part of the midgut corresponding to the copper cell region (referred to as normal) (Figure 5A). In contrast, older flies (21d old) often lose the acidic zone with the entire gut turning either basic (referred to as alkaline) or acidic (referred to as acidic). We estimated the proportion of normal, alkaline, and acidic guts in wild-type and *PGRP-SD^{sk1}* young (3-5d old) and 21d old flies. To do this, we fed each group of flies overnight on food supplemented with bromophenol blue dye, dissected their guts and determined the pH category based on colour (see representative images in Figure 5A). No difference was observed in young flies. However, nearly all the intestines of 21d old *PGRP-SD^{sk1}* mutants were acidic (Figure 5B). Of note, raising *PGRP-SD^{sk1}* flies in germ-free conditions reduced the proportion of flies with acidic guts, suggesting that *Lp* is responsible for the gut acidification during aging (Figure 5B). A corollary of this hypothesis is that old wild-type

flies with acidic guts should have higher *Lp* loads compared to those with alkaline guts. Indeed, when we dissected the guts from 21d old wild-type flies and estimated bacterial loads by qPCR in alkaline and acidic guts separately, we detected significantly more *Lp,* but not *Acetobacter,* in the acidic guts compared to alkaline ones of conventional wild-type flies (Figure 5C).

Lactic acid produced by *Lp* is the cause of gut acidification and dysplasia

We next investigated whether lactic acid itself is responsible for the gut acidification. A first indication for this came from the measurements of lactate concentration in the guts. We detected nearly twice more lactate in conventionally-raised *PGRP-SD^{sk1}* mutant compared to wild-type flies (Figure 5D), which likely reflects the increased *Lp* load in the mutant. Consistent with this, lactate levels were significantly lower when flies were raised in germ-free conditions. Next, we colonized axenic flies with a mutant strain of *Lp* (*Lp^{TF103}*), which is unable to produce lactic acid (Ferain et al., 1996), but is able to persist in the gut and fly food in similar quantities as *Lp^{WT}* (Figure S3I, J). Acidic guts were retrieved less frequently from flies colonized with *Lp^{TF103}* as compared to those colonized with a wild-type strain, *Lp^{WT}*(Figure 5E). Next, we noticed that *PGRP-SD^{sk1}* mutant colonized with *Lp^{TF103}* lives significantly longer compared to flies colonized with *Lp^{WT}* (Figure 5F). *Lp^{TF103}* mono-colonized flies had decreased ROS levels, establishing a link between lactic acid and ROS production (Figure 5G). Additionally, *upd3* expression, a readout of the JAK-STAT pathway, was reduced in flies colonized with *Lp^{TF103}* compared to flies colonized with *Lp^{WT}* (Figure 5H). In line with this, *Lp^{TF103}* colonized flies had decreased ISC proliferation as estimated by PH3 counts (Figure 5I). These results suggest that commensal-derived lactic acid contributes to the age-related changes observed in *PGRP-SD^{sk1}* mutants. We therefore compared the lifespan of wild-type axenic flies maintained on standard medium to flies maintained on medium supplemented with L-lactic acid. Flies had a shorter lifespan when kept on L-lactic acid-supplemented medium (Figure 5J) and showed all the intestinal aging hallmarks, including elevated levels of ROS, increased JAK-STAT pathway activation and increased ISC proliferation (Figure S5A-C). Thus, treatment of flies with L-lactic acid recapitulates the phenotypes observed with flies colonized with *Lp*. In addition, blockage of monocarboxylate transporters required for lactate transport with cinnamate (Poole and Halestrap, 1993) could significantly extend the lifespan of *PGRP-SD^{sk1}* mutant flies and reduce dysplasia, indicating that exogenous microbial lactate needs to enter the intestinal cells to induce ROS production (Figure S5D-E).

Host Lactate dehydrogenase is required for *Lp*-mediated generation of ROS

We next investigated how the elevated production of lactic acid contributes to ROS generation by Nox. Lactate triggers ROS production in rat male germ cells and in human leukemic cells via a mechanism involving the oxidation of lactate to pyruvate by Lactate Dehydrogenase (Ldh), which is accompanied by the transformation of NAD+ to NADH (Figure 6A) (Galardo et al., 2014; Luo et al., 2017). Then, NADH can be used by the NADPH-oxidase Nox to generate ROS. We interrogated the relevance of this pathway in *Drosophila*. Genetic silencing of *Ldh* by RNAi specifically in the gut was sufficient to partially rescue all the aging hallmarks of *PGRP-SD^{sk1}* mutants colonized with *Lp^{SD}*, including the higher levels of ROS, PH3 counts, and *upd3* expression (Figure 6B-D). Moreover, the lifespan of *PGRP-SD^{sk1}* mutants was significantly extended upon *Ldh* RNAi (Figure 6E). Additionally, we explored the lifespan of *Ldh RNAi* flies exposed specifically to L-lactic acid. We observed that *Ldh RNAi* flies live significantly longer on L-lactic supplemented food compared to control flies (Figure 6F). Moreover, feeding flies with oxamate, an inhibitor of Ldh, (Gillis et al., 2018), rescues all the aging hallmarks of *PGRP-SD^{sk1}* flies and

extends their lifespan (Figure S6A-D). In *Drosophila* there is only one Ldh that can convert only L but not D isomer of lactic acid. This implies that D-lactic acid should not be able to induce ROS as it cannot be utilized by the *Drosophila* Ldh. Consistent with this, D-lactic acid did not induce ROS, dysplasia and lifespan shortening in flies in contrast to L isomer (Figure 5J, S5A-C). These findings provide evidences supporting a central role of Ldh in ROS generation by *Lp*, likely by oxidizing L-lactate and generating NADH, a substrate for *Nox*.

PGRP-SD overexpression prevents dysbiosis and extends lifespan

Finally, we explored whether the overexpression of *PGRP-SD* could rescue aging-related pathologies of wild-type flies. Using the *UAS-PGRP-SD* transgene, we observed that gut-specific (*Myo1A-Gal4* driver) *PGRP-SD* overexpression extends the lifespan of flies (Figure 7A). This effect is likely due to reduced dysbiosis in these flies, as *PGRP-SD* over-expression reduced *Lp* counts (Figure 7B). We also detected a lower amount of ROS in *PGRP-SD*-overexpressing flies (Figure 7C). Other aging hallmarks, like increased dysplasia (PH3 counts) and higher JAK-STAT pathway activity (*upd3* expression) were also suppressed upon *PGRP-SD* overexpression (Figure 7D-E). These results identify PGRP-SD as a key factor maintaining intestinal homeostasis and required for optimal longevity.

Discussion

The mucosal immune system uses multiple complex mechanisms to maintain a balance between preserving a beneficial microbiota and eliminating pathogens. This dynamic between immune system and microbiota undergoes age-related changes in animals, including humans (Heintz and Mair, 2014). In *Drosophila*, aging is associated with a series of hallmarks: a higher microbiota load, an increased immune response, elevated ROS, dysplasia, loss of compartmentalization and rupture of barrier permeability (Biteau et al., 2010; Buchon et al., 2009b; Clark et al., 2015; Guo et al., 2014; Li et al., 2016). Interestingly, precocious intestinal senescence equally affects mutants with immune over-activation (ex. *Caudal, PGRP-LB*) and immune deficiency (*Relish, Foxo*) (Buchon et al., 2009b; Paredes et al., 2011; Ryu et al., 2008). However, causal relationships between immune dysfunction, dysbiosis and dysplasia are not clearly established. Here, we used *PGRP-SD*^{sk1} mutant flies with reduced immune reactivity as a tool to characterize a pathway linking immune deficiency to precocious intestinal aging. We found that immune-deficient flies carried increased loads of the dominant microbiota member, *Lp*, which led to a higher release of lactate/lactic acid. This bacterial metabolite not only acidified the intestine, but also stimulated ROS production by NOX, which triggered precocious aging. Our model is appealing for two reasons. First, it does not involve a change in the microbiota composition per se, but rather an overgrowth of a common, preexisting microbiota member. Second, it shows how a bacterial metabolite, lactate, when processed by the host epithelia, drives ROS production and intestinal senescence. This model is likely to apply to other contexts, including mammalian gut microbiota.

Previously, we identified PGRP-SD as a major immune sensor implicated in systemic immunity. In the present study, we uncovered the central function PGRP-SD plays in intestinal immunity, notably by inducing an efficient immune response to pathogens while promoting tolerance to microbiota. This differential response is due to its ability to control the expression of negative regulators that confer immune tolerance. By controlling the local expression of negative regulators of IMD pathway activity, PGRP-SD might prevent the systemic spread of immune activation, a function similar to that of PGRP-LE (Bosco-Drayon et al., 2012).

Numerous studies have reported an increase in total microbiota load in the gut upon aging, and speculated that this change contributes to host mortality, as elimination of microbiota often prolongs lifespan (Broderick et al., 2014; Buchon et al., 2009b; Clark et al., 2015; Guo et al., 2014; Li et al., 2016). It remained unclear whether increased microbiota loads caused accelerated ageing directly or rather indirectly, by inducing chronic immune activation in the gut. Our study answers this question by proving that the *PGRP-SD*^{sk1} mutant, which has increased microbiota loads but is incapable of chronic immune activation, still displays hallmarks of accelerated aging. Our findings unravel a direct causal mechanism linking increases in bacterial loads to gut senescence. Specifically, we showed that aging *PGRP-SD*^{sk1} mutants lose control over their microbial communities, resulting in increased microbiota loads dominated by *Lactobacillus*. The *Lp*-derived metabolite lactic acid/lactate stimulated ROS production by the NADPH oxidase Nox. Our model is supported by the observation that a lactic acid-deficient *Lp* strain did not cause any precocious aging in *PGRP-SD*^{sk1} mutants. Moreover, feeding flies with lactic acid was sufficient to recapitulate all the aging hallmarks caused by *Lp*. Importantly, lactate produced by the symbionts needed to enter and be processed in host cells to activate NOX. This was supported by the observation that inactivating the host's lactate dehydrogenase or the lactate transporters in enterocytes suppressed *Lp*- or lactic acid-mediated dysplasia and lifespan shortening.

In other contexts, dysbiosis with a change in microbiota composition, has been recognized as a contributing factor to epithelial dysplasia, immune-senescence and age-related mortality (Clark et al., 2015; Guo et al., 2014; Li et al., 2016). For example, flies with reduced *Caudal* expression and high IMD pathway activity favor the growth of the pathobiont *Gluconobacter EW707*, which drives host mortality (Ryu et al., 2008). In contrast, we did not find changes in microbiota composition between *PGRP-SD*^{sk1} mutant and wild-type flies, excluding the possibility that immune defects in *PGRP-SD*^{sk1} mutants favor the selection of pathobionts. Thus, excessively increased loads of an otherwise beneficial *Lp* symbiont in *PGRP-SD*^{sk1} flies seem to be solely responsible for the lifespan shortening.

Of note, mammalian PGRPs have also been implicated in the regulation of microbiota composition. Mice deficient for any of the four PGRPs (Pglyrp1-4) are more sensitive to colitis than wild-type mice due to a more inflammatory microbiota (Saha et al., 2010). This points to a conserved role of PGRPs as modulators of host-microbe interactions in the gut.

Moreover, our finding that a commensal bacterium becomes detrimental in the immunocompromised background holds true for mammals as well. For instance, *Lactobacilli* that are beneficial members of human gut microbiota (van Baarlen et al., 2013; Huttenhower et al., 2012) were associated with diseases like D-lactic acidosis, bacteremia, endocarditis and localized infections (Cannon et al., 2005; Vitetta et al., 2017). Whereas these cases are rare and predominantly occurred in immunocompromised individuals, they raise awareness of the good microbe stereotype. As recently pointed out, whether the microbe is helpful or harmful is a question of context and involves a variety of host and microbial factors (Cirstea et al., 2018).

Currently, there is a growing appreciation of how bacterial metabolites affect host physiology (Nicholson et al., 2012). Here, we identified *Lp*-derived lactic acid as an essential metabolite triggering Nox-dependent ROS production and ISCs proliferation. In this context, it would be interesting to test whether the same process, lactate production by the indigenous microbiota, can drive ROS production by Nox in mammals. While formal evidence is still lacking, this is likely to be the case. Indeed, *L. murinus*-derived lactate was found to accelerate colon epithelial turnover

in starvation-refed mice, although the role of ROS was not assessed (Okada et al., 2013). Other complementary studies have shown that *Lp* induces Nox-dependent ISC proliferation in the mammalian intestine as well (Jones et al., 2013), but whether lactic acid mediates this effect was not tested. Collectively, our results and these studies suggest a conserved mechanism of Nox activation by lactate which couples bacterial growth to ISC proliferation.

In *Drosophila* two enzymes, Nox and Duox, can generate ROS and trigger ISC proliferation in response to microbes. Consistent with previous studies, we found here that induction of ROS by *Lp* required Nox but not Duox (Jones et al., 2013). We further showed that Nox was activated by microbiota-derived lactate, whereas Duox is activated by pathogen-released uracil (Lee et al., 2013). Although both lactate and uracil ultimately activate ROS production, they may have contrasting roles in host metabolism. Duox-generated ROS primarily serve to eliminate pathogens and induce regeneration to repair acute, infection-induced damage, while Nox-derived ROS ensure a basal homeostatic level of epithelial renewal in response to microbiota. The fact that both oxidases are expressed in different regions and cell types of the gut further supports functional differences of these two enzymes (Dutta et al., 2015). This would explain why NADH, which is produced by lactate oxidation and is a substrate for both Nox and Duox, induces ROS exclusively in a Nox-dependent manner.

In conclusion, we have discovered a fascinating example of interspecies metabolic crosstalk, where a microbe-derived metabolite is transformed by the host enzymes into a molecule affecting epithelium turnover and host lifespan. While microbial metabolites affecting host lifespan have been described before (Gusarov et al., 2013; Heintz and Mair, 2014), the exact mechanism was rarely identified. Our results establish a direct link between microbiota overgrowth and dysplasia, while revealing the importance of host-microbe metabolic crosstalk in promoting age-related pathologies. Further elucidation of the molecular relationship between the immune system, dysbiosis and host physiology may open up promising avenues for healthy aging.

Acknowledgments

We thank the Bloomington Stock Centre and the Vienna Drosophila Resource Center for fly stocks, Won-Jae Lee and Pascal Hols for providing *L. plantarum* strains. We are grateful to Claudine Neyen for critical reading of the manuscript. This project was supported by the SNSF grant 3100A0-12079/1.

Author contributions

I.I. and B.L. designed the study and wrote the manuscript. I.I. performed most of the experiments. J.-P.B. conducted immunostaining experiments.

Declaration of interest

The authors declare no competing interests.

References

Aggarwal, K., Rus, F., Vriesema-Magnuson, C., Ertürk-Hasdemir, D., Paquette, N., and Silverman, N. (2008). Rudra Interrupts Receptor Signaling Complexes to Negatively Regulate the IMD Pathway. PLoS Pathog. *4*, e1000120.

Apidianakis, Y., and Rahme, L.G. (2011). Drosophila melanogaster as a model for human intestinal infection and pathology. Dis. Model. Mech. *4*, 21–30.

van Baarlen, P., Wells, J.M., and Kleerebezem, M. (2013). Regulation of intestinal homeostasis and immunity with probiotic lactobacilli. Trends Immunol. *34*, 208–215.

Bae, Y.S., Choi, M.K., and Lee, W.-J. (2010). Dual oxidase in mucosal immunity and host–microbe homeostasis. Trends Immunol. *31*, 278–287.

Basset, A., Khush, R.S., Braun, A., Gardan, L., Boccard, F., Hoffmann, J.A., and Lemaitre, B. (2000). The phytopathogenic bacteria Erwinia carotovora infects Drosophila and activates an immune response. Proc. Natl. Acad. Sci. *97*, 3376–3381.

Biteau, B., Karpac, J., Supoyo, S., DeGennaro, M., Lehmann, R., and Jasper, H. (2010). Lifespan Extension by Preserving Proliferative Homeostasis in Drosophila. PLoS Genet. *6*, e1001159.

Biteau, B., Hochmuth, C.E., and Jasper, H. (2011). Maintaining Tissue Homeostasis: Dynamic Control of Somatic Stem Cell Activity. Cell Stem Cell *9*, 402–411.

Blum, J.E., Fischer, C.N., Miles, J., and Handelsman, J. (2013). Frequent replenishment sustains the beneficial microbiome of Drosophila melanogaster. MBio *4*, e00860-13.

Bosco-Drayon, V., Poidevin, M., Boneca, I.G., Narbonne-Reveau, K., Royet, J., and Charroux, B. (2012). Peptidoglycan sensing by the receptor PGRP-LE in the Drosophila gut induces immune responses to infectious bacteria and tolerance to microbiota. Cell Host Microbe *12*, 153–165.

Broderick, N.A., and Lemaitre, B. (2012). Gut-associated microbes of Drosophila melanogaster. Gut Microbes *3*, 307–321.

Broderick, N.A., Buchon, N., and Lemaitre, B. (2014). Microbiota-induced changes in drosophila melanogaster host gene expression and gut morphology. MBio *5*, e01117-14.

Buchon, N., Broderick, N.A., Poidevin, M., Pradervand, S., and Lemaitre, B. (2009a). Drosophila Intestinal Response to Bacterial Infection: Activation of Host Defense and Stem Cell Proliferation. Cell Host Microbe *5*, 200–211.

Buchon, N., Broderick, N.A., Chakrabarti, S., and Lemaitre, B. (2009b). Invasive and indigenous microbiota impact intestinal stem cell activity through multiple pathways in Drosophila. Genes Dev. *23*, 2333–2344.

Buchon, N., Broderick, N.A., and Lemaitre, B. (2013). Gut homeostasis in a microbial world: insights from Drosophila melanogaster. Nat. Rev. Microbiol. *11*, 615–626.

Cannon, J.P., Lee, T.A., Bolanos, J.T., and Danziger, L.H. (2005). Pathogenic relevance of Lactobacillus: a retrospective review of over 200 cases. Eur. J. Clin. Microbiol. Infect. Dis. *24*, 31–40.

Capo, F., Charroux, B., and Royet, J. (2016). Bacteria sensing mechanisms in Drosophila gut: Local and systemic consequences. Dev. Comp. Immunol. *64*, 11–21.

Charroux, B., Capo, F., Kurz, C.L., Peslier, S., Chaduli, D., Viallat-Lieutaud, A., and Royet, J. (2018). Cytosolic and Secreted Peptidoglycan-Degrading Enzymes in Drosophila Respectively

Control Local and Systemic Immune Responses to Microbiota. Cell Host Microbe *23*, 215–228.e4.

Choi, N.-H., Kim, J.-G., Yang, D.-J., Kim, Y.-S., and Yoo, M.-A. (2008). Age-related changes in Drosophila midgut are associated with PVF2, a PDGF/VEGF-like growth factor. Aging Cell *7*, 318–334.

Cirstea, M., Radisavljevic, N., and Finlay, B.B. (2018). Good Bug, Bad Bug: Breaking through Microbial Stereotypes. Cell Host Microbe *23*, 10–13.

Clark, R.I., Salazar, A., Yamada, R., Fitz-Gibbon, S., Morselli, M., Alcaraz, J., Rana, A., Rera, M., Pellegrini, M., Ja, W.W., et al. (2015). Distinct Shifts in Microbiota Composition during Drosophila Aging Impair Intestinal Function and Drive Mortality. Cell Rep. *12*, 1656–1667.

Clemente, J.C., Ursell, L.K., Parfrey, L.W., and Knight, R. (2012). The Impact of the Gut Microbiota on Human Health: An Integrative View. Cell *148*, 1258–1270.

Dutta, D., Dobson, A.J., Houtz, P.L., Gläßer, C., Revah, J., Korzelius, J., Patel, P.H., Edgar, B.A., and Buchon, N. (2015). Regional Cell-Specific Transcriptome Mapping Reveals Regulatory Complexity in the Adult Drosophila Midgut. Cell Rep. *12*, 346–358.

Ferain, T., Hobbs, J.N., Richardson, J., Bernard, N., Garmyn, D., Hols, P., Allen, N.E., and Delcour, J. (1996). Knockout of the two ldh genes has a major impact on peptidoglycan precursor synthesis in Lactobacillus plantarum. J. Bacteriol. *178*, 5431–5437.

Fink, C., Hoffmann, J., Knop, M., Li, Y., Isermann, K., and Roeder, T. (2016). Intestinal FoxO signaling is required to survive oral infection in Drosophila. Mucosal Immunol. *9*, 927–936.

Galardo, M.N., Regueira, M., Riera, M.F., Pellizzari, E.H., Cigorraga, S.B., and Meroni, S.B. (2014). Lactate Regulates Rat Male Germ Cell Function through Reactive Oxygen Species. PLoS One *9*, e88024.

Garrett, W.S., Gordon, J.I., and Glimcher, L.H. (2010). Homeostasis and Inflammation in the Intestine. Cell *140*, 859–870.

Gillis, C.C., Hughes, E.R., Spiga, L., Winter, M.G., Zhu, W., Furtado de Carvalho, T., Chanin, R.B., Behrendt, C.L., Hooper, L. V, Santos, R.L., et al. (2018). Dysbiosis-Associated Change in Host Metabolism Generates Lactate to Support Salmonella Growth. Cell Host Microbe *23*, 54–64.e6.

Guo, L., Karpac, J., Tran, S.L., and Jasper, H. (2014). PGRP-SC2 promotes gut immune homeostasis to limit commensal dysbiosis and extend lifespan. Cell *156*, 109–122.

Gusarov, I., Gautier, L., Smolentseva, O., Shamovsky, I., Eremina, S., Mironov, A., and Nudler, E. (2013). Bacterial nitric oxide extends the lifespan of C. elegans. Cell *152*, 818–830.

Ha, E.-M., Oh, C.-T., Bae, Y.S., and Lee, W.-J. (2005). A direct role for dual oxidase in Drosophila gut immunity. Science *310*, 847–850.

Heintz, C., and Mair, W. (2014). You are what you host: microbiome modulation of the aging process. Cell *156*, 408–411.

Hochmuth, C.E., Biteau, B., Bohmann, D., and Jasper, H. (2011). Redox Regulation by Keap1

and Nrf2 Controls Intestinal Stem Cell Proliferation in Drosophila. Cell Stem Cell *8*, 188–199.

Hooper, L. V, and Gordon, J.I. (2001). Commensal host-bacterial relationships in the gut. Science *292*, 1115–1118.

Huttenhower, C., Gevers, D., Knight, R., Abubucker, S., Badger, J.H., Chinwalla, A.T., Creasy, H.H., Earl, A.M., FitzGerald, M.G., Fulton, R.S., et al. (2012). Structure, function and diversity of the healthy human microbiome. Nature *486*, 207–214.

Iatsenko, I., Kondo, S., Mengin-Lecreulx, D., and Lemaitre, B. (2016). PGRP-SD, an Extracellular Pattern-Recognition Receptor, Enhances Peptidoglycan-Mediated Activation of the Drosophila Imd Pathway. Immunity *45*, 1013–1023.

Jiang, H., Patel, P.H., Kohlmaier, A., Grenley, M.O., McEwen, D.G., and Edgar, B.A. (2009). Cytokine/Jak/Stat Signaling Mediates Regeneration and Homeostasis in the Drosophila Midgut. Cell *137*, 1343–1355.

Jones, R.M., Luo, L., Ardita, C.S., Richardson, A.N., Kwon, Y.M., Mercante, J.W., Alam, A., Gates, C.L., Wu, H., Swanson, P.A., et al. (2013). Symbiotic lactobacilli stimulate gut epithelial proliferation via Nox-mediated generation of reactive oxygen species. EMBO J. *32*, 3017–3028.

Kaneko, T., Goldman, W.E., Mellroth, P., Steiner, H., Fukase, K., Kusumoto, S., Harley, W., Fox, A., Golenbock, D., and Silverman, N. (2004). Monomeric and Polymeric Gram-Negative Peptidoglycan but Not Purified LPS Stimulate the Drosophila IMD Pathway. Immunity *20*, 637–649.

Kleino, A., and Silverman, N. (2014). The Drosophila IMD pathway in the activation of the humoral immune response. Dev. Comp. Immunol. *42*, 25–35.

Kleino, A., Myllymäki, H., Kallio, J., Vanha-aho, L.-M., Oksanen, K., Ulvila, J., Hultmark, D., Valanne, S., and Rämet, M. (2008). Pirk is a negative regulator of the Drosophila Imd pathway. J. Immunol. *180*, 5413–5422.

Kleino, A., Ramia, N.F., Bozkurt, G., Shen, Y., Nailwal, H., Huang, J., Napetschnig, J., Gangloff, M., Chan, F.K.-M., Wu, H., et al. (2017). Peptidoglycan-Sensing Receptors Trigger the Formation of Functional Amyloids of the Adaptor Protein Imd to Initiate Drosophila NF-κB Signaling. Immunity *47*, 635–647.e6.

Kuraishi, T., Binggeli, O., Opota, O., Buchon, N., and Lemaitre, B. (2011). Genetic evidence for a protective role of the peritrophic matrix against intestinal bacterial infection in Drosophila melanogaster. Proc. Natl. Acad. Sci. U. S. A. *108*, 15966–15971.

Lee, K.-A., Kim, S.-H., Kim, E.-K., Ha, E.-M., You, H., Kim, B., Kim, M.-J., Kwon, Y., Ryu, J.-H., and Lee, W.-J. (2013). Bacterial-Derived Uracil as a Modulator of Mucosal Immunity and Gut-Microbe Homeostasis in Drosophila. Cell *153*, 797–811.

Lemaitre, B., and Hoffmann, J. (2007). The Host Defense of Drosophila melanogaster. Annu. Rev. Immunol. *25*, 697–743.

Ley, R.E., Peterson, D.A., and Gordon, J.I. (2006). Ecological and Evolutionary Forces Shaping Microbial Diversity in the Human Intestine. Cell *124*, 837–848.

Lhocine, N., Ribeiro, P.S., Buchon, N., Wepf, A., Wilson, R., Tenev, T., Lemaitre, B., Gstaiger, M., Meier, P., and Leulier, F. (2008). PIMS Modulates Immune Tolerance by Negatively Regulating Drosophila Innate Immune Signaling. Cell Host Microbe *4*, 147–158.

Li, H., Qi, Y., and Jasper, H. (2016). Preventing Age-Related Decline of Gut Compartmentalization Limits Microbiota Dysbiosis and Extends Lifespan. Cell Host Microbe *19*, 240–253.

Liu, X., Hodgson, J.J., and Buchon, N. (2017). Drosophila as a model for homeostatic, antibacterial, and antiviral mechanisms in the gut. PLOS Pathog. *13*, e1006277.

Luo, S.-T., Zhang, D.-M., Qin, Q., Lu, L., Luo, M., Guo, F.-C., Shi, H.-S., Jiang, L., Shao, B., Li, M., et al. (2017). The Promotion of Erythropoiesis via the Regulation of Reactive Oxygen Species by Lactic Acid. Sci. Rep. *7*, 38105.

Martino, M., Ma, D., and Leulier, F. (2017). Microbial influence on Drosophila biology. Curr. Opin. Microbiol. *38*, 165–170.

Monahan, A., Kleino, A., and Silverman, N. (2016). ReaDAPting the Role of PGRP-SD in Bacterial Sensing and Immune Activation. Immunity *45*, 951–953.

Neyen, C., Poidevin, M., Roussel, A., and Lemaitre, B. (2012). Tissue- and ligand-specific sensing of gram-negative infection in drosophila by PGRP-LC isoforms and PGRP-LE. J. Immunol. *189*, 1886–1897.

Nicholson, J.K., Holmes, E., Kinross, J., Burcelin, R., Gibson, G., Jia, W., and Pettersson, S. (2012). Host-gut microbiota metabolic interactions. Science *336*, 1262–1267.

Okada, T., Fukuda, S., Hase, K., Nishiumi, S., Izumi, Y., Yoshida, M., Hagiwara, T., Kawashima, R., Yamazaki, M., Oshio, T., et al. (2013). Microbiota-derived lactate accelerates colon epithelial cell turnover in starvation-refed mice. Nat. Commun. *4*, 1654.

Overend, G., Luo, Y., Henderson, L., Douglas, A.E., Davies, S.A., and Dow, J.A.T. (2016). Molecular mechanism and functional significance of acid generation in the Drosophila midgut. Sci. Rep. *6*, 27242.

Pais, I.S., Valente, R.S., Sporniak, M., and Teixeira, L. (2018). Drosophila melanogaster establishes a species-specific mutualistic interaction with stable gut-colonizing bacteria. PLOS Biol. *16*, e2005710.

Paredes, J.C., Welchman, D.P., Poidevin, M., and Lemaitre, B. (2011). Negative regulation by amidase PGRPs shapes the Drosophila antibacterial response and protects the fly from innocuous infection. Immunity *35*, 770–779.

Pfeiler, E.A., and Klaenhammer, T.R. (2007). The genomics of lactic acid bacteria. Trends Microbiol. *15*, 546–553.

Poole, R.C., and Halestrap, A.P. (1993). Transport of lactate and other monocarboxylates across mammalian plasma membranes. Am. J. Physiol. *264*, C761-82.

Ryu, J.-H., Kim, S.-H., Lee, H.-Y., Bai, J.Y., Nam, Y.-D., Bae, J.-W., Lee, D.G., Shin, S.C., Ha, E.-M., and Lee, W.-J. (2008). Innate immune homeostasis by the homeobox gene caudal and

commensal-gut mutualism in Drosophila. Science *319*, 777–782.

Ryu, J.H., Ha, E.M., Oh, C.T., Seol, J.H., Brey, P.T., Jin, I., Lee, D.G., Kim, J., Lee, D., and Lee, W.J. (2006). An essential complementary role of NF-κB pathway to microbicidal oxidants in Drosophila gut immunity. EMBO J. *25*, 3693–3701.

Saha, S., Jing, X., Park, S.Y., Wang, S., Li, X., Gupta, D., and Dziarski, R. (2010). Peptidoglycan recognition proteins protect mice from experimental colitis by promoting normal gut flora and preventing induction of interferon-gamma. Cell Host Microbe *8*, 147–162.

Sannino, D.R., Dobson, A.J., Edwards, K., Angert, E.R., and Buchon, N. (2018). The Drosophila melanogaster Gut Microbiota Provisions Thiamine to Its Host. MBio *9*, e00155-18.

Sekihara, S., Shibata, T., Hyakkendani, M., and Kawabata, S. (2016). RNA Interference Directed against the *Transglutaminase* Gene Triggers Dysbiosis of Gut Microbiota in *Drosophila*. J. Biol. Chem. *291*, 25077–25087.

Sharon, G., Segal, D., Ringo, J.M., Hefetz, A., Zilber-Rosenberg, I., and Rosenberg, E. (2010). Commensal bacteria play a role in mating preference of Drosophila melanogaster. Proc. Natl. Acad. Sci. U. S. A. *107*, 20051–20056.

Storelli, G., Defaye, A., Erkosar, B., Hols, P., Royet, J., and Leulier, F. (2011). Lactobacillus plantarum Promotes Drosophila Systemic Growth by Modulating Hormonal Signals through TOR-Dependent Nutrient Sensing. Cell Metab. *14*, 403–414.

Storelli, G., Strigini, M., Grenier, T., Bozonnet, L., Schwarzer, M., Daniel, C., Matos, R., and Leulier, F. (2018). Drosophila Perpetuates Nutritional Mutualism by Promoting the Fitness of Its Intestinal Symbiont Lactobacillus plantarum. Cell Metab. *27*, 362–377.e8.

Tzou, P., Ohresser, S., Ferrandon, D., Capovilla, M., Reichhart, J.-M., Lemaitre, B., Hoffmann, J.A., and Imler, J.-L. (2000). Tissue-Specific Inducible Expression of Antimicrobial Peptide Genes in Drosophila Surface Epithelia. Immunity *13*, 737–748.

Vitetta, L., Coulson, S., Thomsen, M., Nguyen, T., and Hall, S. (2017). Probiotics, D–Lactic acidosis, oxidative stress and strain specificity. Gut Microbes *8*, 311–322.

Vodovar, N., Vinals, M., Liehl, P., Basset, A., Degrouard, J., Spellman, P., Boccard, F., and Lemaitre, B. (2005). Drosophila host defense after oral infection by an entomopathogenic Pseudomonas species. Proc. Natl. Acad. Sci. U. S. A. *102*, 11414–11419.

Wong, A.C.-N., Chaston, J.M., and Douglas, A.E. (2013). The inconstant gut microbiota of Drosophila species revealed by 16S rRNA gene analysis. ISME J. *7*, 1922–1932.

Wong, C.N.A., Ng, P., and Douglas, A.E. (2011). Low-diversity bacterial community in the gut of the fruitfly Drosophila melanogaster. Environ. Microbiol. *13*, 1889–1900.

Xu, C., Luo, J., He, L., Montell, C., and Perrimon, N. (2017). Oxidative stress induces stem cell proliferation via TRPA1/RyR-mediated Ca2+ signaling in the Drosophila midgut. Elife *6*, e22441.

Zaidman-Rémy, A., Hervé, M., Poidevin, M., Pili-Floury, S., Kim, M.-S., Blanot, D., Oh, B.-H., Ueda, R., Mengin-Lecreulx, D., and Lemaitre, B. (2006). The Drosophila Amidase PGRP-LB

Modulates the Immune Response to Bacterial Infection. Immunity *24*, 463–473.

Zhai, Z., Boquete, J.-P., and Lemaitre, B. (2018). Cell-Specific Imd-NF-κB Responses Enable Simultaneous Antibacterial Immunity and Intestinal Epithelial Cell Shedding upon Bacterial Infection. Immunity *48*, 897–910.e7.

Figure legends

Figure 1. PGRP-SD is required in the gut for IMD pathway activation and protection against pathogens

(A) RT-qPCR showing *PGRP-SD* expression in midguts of flies of indicated genotypes after *Ecc15* oral infection.
(B) Schematic representation of PGRP-SD promoter region.
(C) Immunostaining showing PGRP-SD localization in the gut under unchallenged (UC) and infected (*Ecc15*) conditions.
(D) RT-qPCR showing *Dpt* expression in midguts of wild-type, *PGRP-SD^{sk1}* mutant and *PGRP-SD^{sk1}* mutant over deficiency after *Ecc15* oral infection.
(E) RT-qPCR of *Dpt* expression in midguts after tissue- and cell- specific silencing of *PGRP-SD* by RNAi. *Dpt* expression in *GAL4*-driver stocks crossed with *w^{1118}* was set to 100 and expression in *GAL4* stocks crossed with *UAS-PGRP-SD-IR* was expressed as a percentage of this value.
(F) Tissue-specific rescue of *Dpt* expression in *PGRP-SD^{sk1}* mutants 6 h post oral infection (hpi) with *Ecc15* as measured by RT-qPCR.
(G) Survival rates of flies orally infected with *P. entomophila.*
(H) *PGRP-SD* expression in the midguts of axenic and conventional flies (5d old) measured by RT-qPCR.

(I-K) RT-qPCR of *PGRP-SD* (I), *Dpt* (J), *PGRP-LB* (K) expression in the midguts of axenic and *Lp^{WJL}*-colonized flies 6 h post colonization (hpc).

RT-qPCR results are shown as mean ± s.d. of at least three independent samples (n=20 female midguts per each sample). In 1F *Dpt* levels in infected wild-type flies (6 h) were set to 100 and all other values were expressed as a percentage of this value. See also Figure S1.

Figure 2. *PGRP-SD^{sk1}* mutants are short lived due to microbiota-triggered dysplasia

(A) Lifespan curves of wild-type and *PGRP-SD^{sk1}* mutant male flies under conventional and axenic conditions at 25 ºC.
(B) Patterns of cell proliferation revealed by the expression of *Esg-GAL4,UAS-GFP* reporter. Flies were maintained on standard medium (conventional) or on medium supplemented with antibiotics (axenic) at 29 ºC.
(C) Quantification of PH3-positive cells per midgut of 21d old wild-type and *PGRP-SD^{sk1}* mutant under conventional and axenic conditions at 29 ºC. Mean±s.d of three experiments, n=10 guts per each genotype and experiment.
(D) RT-qPCR detecting *upd3* expression in wild-type and *PGRP-SD^{sk1}* mutant under conventional and axenic conditions at 29 ºC. Results are shown are shown as mean ± s.d. of at least three independent samples (n=20 female midguts per each sample).
(E) Lifespan curves of *PGRP-SD^{sk1}* mutant at 29 ºC upon *upd2* inhibition by RNAi in the gut.

See also Figure S2.

Figure 3. Overgrowth of *Lp* shortens lifespan of *PGRP-SD^{sk1}* mutant

(A) Relative frequency of bacterial 16S rRNA clones from libraries generated from 21d old wild-type and *PGRP-SD^{sk1}* mutant populations aged at 29 ºC.

(B) Counts of culturable bacteria (CFUs) associated with wild-type and *PGRP-SD^{sk1}* mutant aged at 29 ºC. The horizontal bar represents mean value. The single dots represent mean individual CFU counts calculated from pools of n=5 animals.

(C) qPCR detecting levels of bacteria relative to host DNA in 21d old wild-type and *PGRP-SD^{sk1}* mutant flies aged at 29 ºC. The horizontal bar represents mean value. The single dots are mean values from pools of n=5 animals.

(D) RT-qPCR detecting *upd3* expression in axenic and *Lp^{SD}*-colonized 21d old wild-type and *PGRP-SD^{sk1}* mutant midguts. Flies were maintained at 29 ºC. Mean ± s.d. of at least three independent samples (n=20 female midguts per each sample).

(E) Quantification of PH3-positive cells per midgut of 21d old wild-type and *PGRP-SD^{sk1}* mutant under axenic and *Lp^{SD}*-colonized conditions at 29 ºC. Mean±s.d of three experiments, n=10 guts per each genotype and experiment.

(F) Lifespan curves of axenic and *Lp^{SD}*-colonized wild-type and *PGRP-SD^{sk1}* mutant male flies at 29 ºC.

(G) Lifespan of wild-type and *PGRP-SD^{sk1}* mutant flies colonized with their own or heterologous microbiota at 29 ºC.

See also Figure S3.

Figure 4. Induction of ROS by Nox triggers dysplasia in *PGRP-SD^{sk1}* mutant

(A) Levels of ROS in 21d old wild-type and *PGRP-SD^{sk1}* mutant guts under conventional and axenic conditions at 29 ºC. Mean±s.d of four experiments, n=20 guts per each experiment and genotype.

(B) Levels of ROS in 21d old axenic and *Lp^{SD}*-colonized wild-type and *PGRP-SD^{sk1}* mutant guts at 29 ºC. Mean±s.d of three experiments, n=20 guts per each experiment and genotype.

(C) RT-qPCR showing *upd3* expression in 21d old wild-type and *PGRP-SD^{sk1}* flies aged at 29 ºC in the presence or absence of NAC. Mean ± s.d. at least three independent samples (n=20 female midguts per each sample).

(D) Lifespan curves of wild-type and *PGRP-SD^{sk1}* mutant male flies exposed to NAC and untreated controls at 29 ºC.

(E-G) ROS levels (E), *upd3* expression (F) and PH3 counts (G) in *Lp^{SD}*- colonized 21d old flies of indicated genotypes at 29 ºC. Mean±s.d of three experiments, n=20 (E, F), n=10 (G) guts per each genotype and experiment. Asterisks above bars indicate significance relative to *Myo1-GAL4>w1118 Lp^{SD}*.

(H) Lifespan curves of conventional male flies of indicated genotypes at 29 ºC.

See also Figure S4.

Figure 5. *Lp*-derived lactic acid induces ROS, dysplasia and shortens lifespan of flies

(A) Intestines of 21d old flies fed the pH indicator bromophenol blue and maintained at 29 ºC. Three phenotypic categories are shown.

(B) Quantification of the three gut pH phenotypes in flies of indicated conditions and maintained at 29 ºC. Pooled results of two repeats (n=20 guts per condition).
(C) qPCR detecting levels of bacteria relative to host DNA in 21d old wild-type guts that were identified as acidic or alkaline based on bromophenol blue staining. The horizontal bar represents mean value. The single dots are mean values from pools of n=5 animals.
(D) Levels of lactate in axenic (ax) and conventional (CR) wild-type and *PGRP-SD*^{sk1} mutant guts at 29 ºC. Mean±s.d of three experiments, n=20 guts per each genotype and experiment.
(E) Quantification of the three gut pH phenotypes in flies of indicated conditions. Pooled results of two repeats (n=20 guts per condition).
(F) Lifespan curves of wild-type and *PGRP-SD*^{sk1} mutant male flies colonized with wild-type *Lp*^{WT} and lactic acid-deficient mutant *Lp*^{TF103} at 29 ºC.

(G-I) ROS levels (G), *upd3* expression (H) and PH3 counts (I) in 21d old wild-type and *PGRP-SD*^{sk1} mutant guts colonized with *Lp*^{WT} and *Lp*^{TF103}. Flies were aged at 29 ºC. Results are shown as mean±s.d of three experiments, n=20 (G, H), n=10 (I) guts per each genotype and experiment.

(J) Lifespan curves of axenic wild-type and *PGRP-SD*^{sk1} mutant male flies on axenic medium without any acids (- acid) and on an axenic medium supplemented with 50 mM L-lactic acid (+L-lactic acid) or D-lactic acid (+D-lactic acid). Performed at 29 ºC.

See also Figure S5.

Figure 6. Ldh is required for *Lp*-mediated generation of ROS and dysplasia

(A) Scheme illustrating potential mechanism of ROS generation by lactate.

(B-D) ROS levels (B), PH3 counts (C) and *upd3* expression (D) in *Lp*^{SD}- colonized 21d old flies of indicated genotypes at 29 ºC. Mean±s.d of three experiments, n=20 (B, D), n=10 (C) guts per each genotype and experiment. Asterisks above bars indicate significance relative to *Myo1-GAL4>w1118 Lp*^{SD}.

(E) Lifespan curves of *Lp*^{SD}- colonized male flies of indicated genotypes at 29 ºC.
(F) Lifespan curves of male flies of indicated genotypes at 29 ºC exposed to 50 mM L-lactic acid (+L-lactic acid) and untreated controls (-acid).

See also Figure S6.

Figure 7. Overexpression of PGRP-SD extends lifespan and reduces dysbiosis

(A) Lifespan curves of males overexpressing PGRP-SD in enterocytes at 29 ºC.
(B) qPCR detecting *Lp* levels relative to host DNA in 21d old flies overexpressing PGRP-SD. Flies were aged at 29 ºC. The horizontal bar represents mean value. The single dots are mean values from pools of n=5 animals.

(C-E) ROS level (C), PH3 counts (D) and *upd3* expression (E) in 21d old flies overexpressing PGRP-SD and aged at 29 ºC. Mean±s.d of three experiments, n=20 (C, E), n=10 (D) guts per each genotype and experiment.

STAR METHODS

Contact for reagent and resource sharing

Further information and requests for resources and reagents should be directed to and will be fulfilled by the Lead Contact, Bruno Lemaitre (bruno.lemaitre@epfl.ch)

Experimental model and subject details

Drosophila stocks and rearing

Drosophila genotypes used in this study are listed in the Key Resources Table. The stocks were routinely maintained at 25 ºC with 12/12 h dark/light cycles on a standard cornmeal-agar medium (see composition below). Fresh food was prepared weekly to avoid desiccation. Axenic stocks were established by bleaching and cultivating embryos on fresh medium supplemented with a cocktail of four antibiotics (see below) for at least one generation, and then maintained on this medium (Broderick et al., 2014). DrosDel w^{1118} *iso* isogenic flies were used as wild-type controls in this work. Male flies were used for survival and lifespan experiments, females – for all other experiments.

Fly diets used in this study

Standard cornmeal medium: 3.72g agar, 35.28g cornmeal, 35.28g inactivated dried yeast, 16 ml of a 10% solution of methyl- paraben in 85% ethanol, 36 ml fruit juice, 2.9 ml 99% propionic acid for 600 ml.

Cornmeal medium with antibiotics for axenic flies: same composition as above with Ampicillin (50µg/ml), Kanamycin (50µg/ml), Tetracyclin (10µg/ml), and Erythromycin (10µg/ml) added just before pouring the food into vials.

Cornmeal medium with N-acetylcysteine: same composition as a standard medium with 20 mM N-acetylcysteine.

Cornmeal medium with oxamate: same composition as a standard medium with 10 mM oxamate.

Cornmeal medium with cinnamate: same composition as a standard medium with 10 mM alpha-cyano-4-hydroxycinnamic acid.

Cornmeal medium without acid (control for a medium with lactic acid): same composition as a medium with antibiotics omitting propionic acid.

Cornmeal medium with lactic acid: same composition as a medium with antibiotics with 50 mM L-lactic acid or D-lactic acid.

Cornmeal medium with Bromophenol blue sodium (pH indicator): same composition as a standard medium with 2% Bromophenol blue sodium.

Bacterial culture conditions

Bacterial strains used in this study are listed in the Key Resources Table. *Lactobacillus plantarum* strains were cultured in Man, Rogosa and Sharpe (MRS) broth medium overnight at 37 ºC with shaking. Solidified MRS medium was used for estimation of colony forming units (CFUs). *Ecc15* and *P. entomophila* were cultured overnight at 30 ºC with shaking in LB medium. Specific details of doses and procedures are indicated below.

Method details

Generation of *PGRP-SD-GAL4* line

A *PGRP-SD-GAL4* line was generated by cloning a 177 bp sequence upstream of *PGRP-SD* gene into pBPGUw vector followed by PhiC31 integrase-mediated transgenesis, landing site 51C on chromosome 2 (BDSC strain 24482). Several independent lines have been obtained and tested. All lines behaved similarly in experiments.

Generation of axenic stocks

To obtain axenic fly stocks, embryos laid over a 16-h period on grape juice plates were collected from 4- to 10-day-old females. Embryos were rinsed in 1× phosphate-buffered saline (PBS) and transferred to 1.5 ml tubes. All following steps were performed in a sterile hood. Embryos were placed in a 3% solution of sodium hypochlorite for 10 min. The bleach solution was discarded and embryos were rinsed three times in sterile PBS. Embryos were transferred by pipette to tubes with antibiotics-supplemented food in a small amount of 100% ethanol and maintained at 25 °C. Subsequent generations were maintained in parallel to their conventionally reared counterparts by transferring adults to new tubes with antibiotics-supplemented food. The axenic state of flies was routinely assessed by culturing.

Colonization of axenic flies with *L. plantarum*

Axenic adult flies (2-4 day old) were starved for 2 h at 29 °C in an empty fly vial before being flipped to a vial with *L. plantarum*. An overnight culture of *L. plantarum* in MRS was adjusted to O.D.50 and mixed 1:1 with 5% sucrose. This mixture (150 µl) was applied to a filter disk covering food surface of the vial. Flies were incubated at 29 °C till dissection or for 24 h when they were flipped to a fresh vial with standard food. This procedure ensures consistent, simultaneous and persistent colonization of all individual flies (Bosco-Drayon et al., 2012).

Microbiota transplantation

The same procedure as for colonization of axenic flies with *L. plantarum* was followed. Instead of pure bacterial culture, homogenates of 15-20 day old wild-type and *PGRP-SD*^{sk1} mutant flies were used. To obtain homogenates, 5 female flies (wild-type or *PGRP-SD*^{sk1} mutant) were homogenized in 300 µl of MRS medium with a Precellys 24 instrument (Bertin Technologies, France). Fly debris was removed by brief centrifugation and supernatant was mixed with 5% sucrose and applied to filter disk as described above.

ß-galactosidase staining

Adult guts were dissected in PBS, fixed for 10 min in 0.5% glutaraldehyde on ice, washed in PBS, and incubated at 37°C in ß-galactosidase staining buffer (Na2 HPO4 10mM, NaH2PO4 1.6mM, NaCl 150mM, MgCl2 1mM, K3FeCN6 3.5mM, K4FeCN6 3.5mM, X-gal 4mg/mL) for about 15 minutes (Paredes et al., 2011).

Live Imaging and Immunofluorescence

Imaging was performed as previously described (Buchon et al., 2009a). For detection of PH3 positive cells by immunofluorescence, guts were dissected and fixed in PBS containing 0.1%

Tween 20 (PBT) and 4% paraformaldehyde and rinsed in PBT. Guts were incubated with the primary antibody (anti-PH3) diluted in PBT + 1% BSA. Anti-PH3 was revealed with an Alexa555-coupled goat anti-rabbit antibody. Prospero and Dl-lacZ staining was performed similar to PH3, except that antibody dilutions were: 1:100 for anti-Prospero and 1:1000 for anti-lacZ. *Esg-GAL4,UAS-GFP, 10×Stat-GFP*, and *PGRP-SD-GAL4;UAS-GFP* guts were fixed in PBS containing 0.1% Tween 20 (PBT) and 4% paraformaldehyde before microscopy. Nuclei were stained with DAPI (Sigma). For ROS measurement with DHE, guts were dissected and directly incubated in 30 µM DHE (Life Technologies) for 10 min at room temperature, washed twice and mounted for microscopy immediately. *PGRP-SD-GAL4;UAS-GFP* images were obtained using Zeiss LSM700 confocal microscope. All other images were obtained using a Zeiss Axioimager Z1.

Microbiota analysis

(**A**) Culture-independent. Multiple batches of 5 female flies per treatment/genotype were collected from independent experiments and frozen at -20 °C until used for DNA extraction. Total DNA was extracted from whole flies that were surface sterilized for 1 min in 95% ethanol using Puregene kit (Qiagen). Briefly, 5 flies were squashed in 300 µl of cell lysis solution on ice in 1.5 ml tubes using a pestle. After 15 min incubation at 65 °C, 100 µl of protein precipitation solution was added. Samples were vortexed and incubated on ice for 5 minutes. After centrifugation at max speed for 3 mins, the supernatant was transferred to a new tube and DNA was precipitated with 300 µl of isopropanol. DNA was pelleted by centrifugation at max speed for 5 mins and the pellet was washed with 300 µl of 70% ethanol. After drying, DNA was resuspended in 240 µl of DNA hydration solution. This DNA was used for bacterial 16S rRNA amplification with 27F and 1492R primers. TOPO TA cloning kit (Thermo Fisher Scientific) was used to generate clone libraries from obtained PCR amplicons. Clone inserts were PCR amplified and sequenced using the vector primers T7 and M13R. At least 100 clones were analyzed per treatment/genotype. The BLAST sequence analysis tool was used to analyze sequenced clones.

(**B**) Culture-dependent. Quantification of culturable fly-associated bacteria was determined from pools of ten female individuals from the same rearing tube. Flies were surface sterilized in 95% ethanol for 1 min and placed in 200 µl of 1× PBS in a 1.5-ml screw-top microcentrifuge tube containing glass beads. Samples were homogenized using a Precellys 24 instrument (Bertin Technologies, France), and then serial dilutions were made and plated on both Man, Rogosa, and Sharpe (MRS) and mannitol agar and incubated at 25°C. Colonies were counted after 48h. Based on colonies morphological features, two representative isolates were purified. Representative isolates were identified by PCR amplification and sequencing of the 16S rRNA gene. Subsequent quantification was based on designated morphological features with periodic validation by 16S rRNA amplification and sequencing.

(**C**) Using quantitative PCR. Total DNA was extracted from whole flies as described in (A). DNA was diluted three times and 2 µl per reaction were taken for qPCR analysis using a LightCycler 2.0 instrument and the SYBR green I kit (Roche). *Lactobacillus* and *Acetobacter* specific primers and *Drosophila* RP49 primers were used to estimate abundance of each microbes DNA relative to host DNA.

Gut pH estimation

Petri dishes (5 cm) containing fly food supplemented with 2% Bromophenol blue dye (pH indicator) were prepared. Flies were fed overnight on this medium before dissection. Images were taken immediately after each gut was dissected.

RT-qPCR

For quantification of mRNA, whole flies (10) or dissected guts (20) were collected at indicated time points. Total RNA was isolated using TRIzol reagent and dissolved in RNase-free water. Five hundred nanogram total RNA was then reverse-transcribed in 10 µl reaction volume using PrimeScript RT (TAKARA) and random hexamer primers. Quantitative PCR was performed on a LightCycler 480 (Roche) in 96-well plates using the LightCycler® 480 *SYBR Green* I Master Mix. Primer sequences are listed in Key Resources Table and in Table S1.

Oral infection

For adult oral infection, 2–4 day old adults were dehydrated/starved for 2–3 h in empty vials at 29 ºC. After starvation, flies were flipped to an infection vial with standard medium completely covered by a Whatman paper disk. The disk was soaked in control solution (150 µL of 5 % sucrose) or bacterial pellet mixed with control solution (150 µL of sucrose mixture with bacteria). To prepare bacterial pellet, overnight bacterial cultures *(Ecc15* or *P. entomophila)* were concentrated by centrifugation and adjusted to O.D. 200. This adjusted pellet was mixed with sucrose in equal parts and applied to filter disc. Flies were flipped to fresh vials with standard medium next day after infection (Vodovar et al., 2005; Buchon et al., 2009).

Lifespan analysis

All lifespan experiments were performed independently at least three times using 2-3 cohorts of 20 male flies per genotype/treatment each time. Freshly emerged flies were allowed to mate for 2 days at room temperature and sorted according to sex and genotype. Aging experiments were performed at 29 ºC (except Fig. 2A) and flies were flipped to fresh vials every other day. Lifespan experiments with lactic acid were performed under axenic conditions (medium with antibiotics) to eliminate the contribution of microbiota. All other experiments were performed using standard medium and standard media supplemented with different chemicals.

ROS quantification

Amount of ROS in dissected guts (n=20) was estimated using Fluorimetric Hydrogen Peroxide Assay Kit (Sigma) following manufacturer's instructions and was normalized to total protein.

Lactate quantification

Amount of lactate in dissected guts (n=20) was estimated using Lactate Assay Kit (Sigma) following manufacturer's instructions and was normalized to total protein.

Quantification and statistical analysis

Data representation and statistical analysis were performed using GraphPad Prism 6 software. Survival curves were compared using log-rank tests, with Bonferroni corrections for *p* values where multiple comparisons were necessary. All survival and lifespan graphs show one representative experiment out of three independent repeats with 2-3 cohorts of 20 male flies per genotype. Mann-Whitney test was used to analyze data in Figure 1H, 7B-E, S3E. One-way ANOVA was used to analyze data in Figure 1E, 4E-G, 6B-D, S2A, S2C, S5A-C. In all other cases,

Two-way ANOVA was used. Where multiple comparisons were necessary, appropriate Tukey, Dunnett, or Sidak post hoc tests were applied. Other details on statistical analysis can be found in Figure legends. Statistical significance was set at $p \leq 0.05$. Asterisks indicate *$p \leq 0.05$, **$p \leq 0.01$, ***$p \leq 0.001$, ****$p \leq 0.0001$, ns-non-significant, $p > 0.05$.

Figure 1

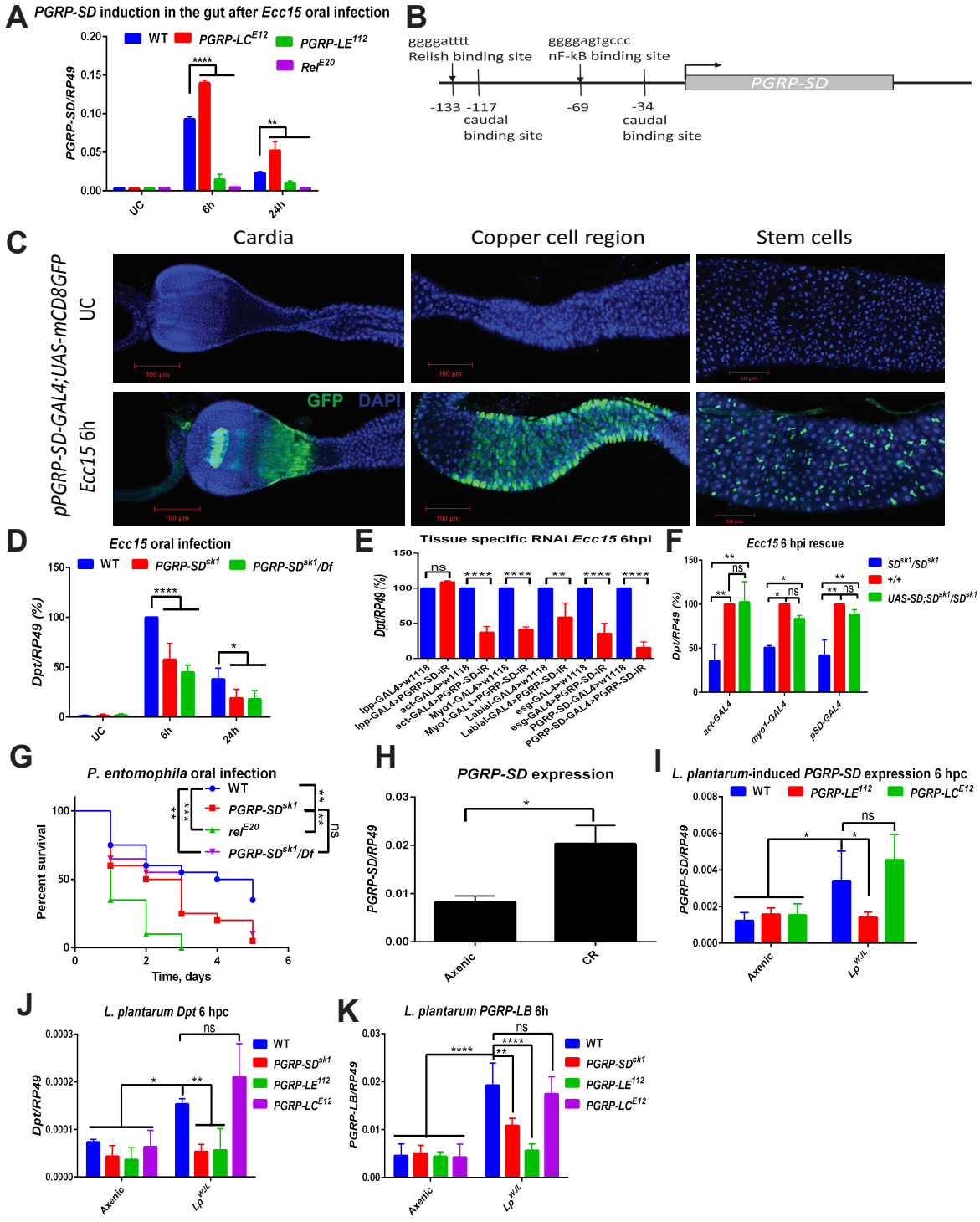
A
PGRP-SD induction in the gut after Ecc15 oral infection
WT
PGRP-LC^E12
PGRP-LE^112
Rel^E20
PGRP-SD/RP49
UC
6h
24h
B
ggggatttt
Relish binding site
ggggagtgccc
nF-kB binding site
PGRP-SD
-133
-117
caudal binding site
-69
-34
caudal binding site
C
Cardia
Copper cell region
Stem cells
pPGRP-SD-GAL4;UAS-mCD8GFP
UC
Ecc15 6h
GFP
DAPI
D
Ecc15 oral infection
WT
PGRP-SD^sk1
PGRP-SD^sk1/Df
Dpt/RP49 (%)
E
Tissue specific RNAi Ecc15 6hpi
Dpt/RP49 (%)
lpp-GAL4>w1118
lpp-GAL4>PGRP-SD-IR
act-GAL4>w1118
act-GAL4>PGRP-SD-IR
Myo1-GAL4>w1118
Myo1-GAL4>PGRP-SD-IR
Labial-GAL4>w1118
Labial-GAL4>PGRP-SD-IR
esg-GAL4>w1118
esg-GAL4>PGRP-SD-IR
PGRP-SD-GAL4>w1118
PGRP-SD-GAL4>PGRP-SD-IR
F
Ecc15 6 hpi rescue
SD^sk1/SD^sk1
+/+
UAS-SD;SD^sk1/SD^sk1
Dpt/RP49 (%)
act-GAL4
myo1-GAL4
pSD-GAL4
G
P. entomophila oral infection
WT
PGRP-SD^sk1
rel^E20
PGRP-SD^sk1/Df
Percent survival
Time, days
H
PGRP-SD expression
PGRP-SD/RP49
Axenic
CR
I
L. plantarum-induced PGRP-SD expression 6 hpc
WT
PGRP-LE^112
PGRP-LC^E12
PGRP-SD/RP49
Axenic
Lp w.t.
J
L. plantarum Dpt 6 hpc
WT
PGRP-SD^sk1
PGRP-LE^112
PGRP-LC^E12
Dpt/RP49
Axenic
Lp w.t.
K
L. plantarum PGRP-LB 6h
WT
PGRP-SD^sk1
PGRP-LE^112
PGRP-LC^E12
PGRP-LB/RP49
Axenic
Lp w.t.

Figure 2

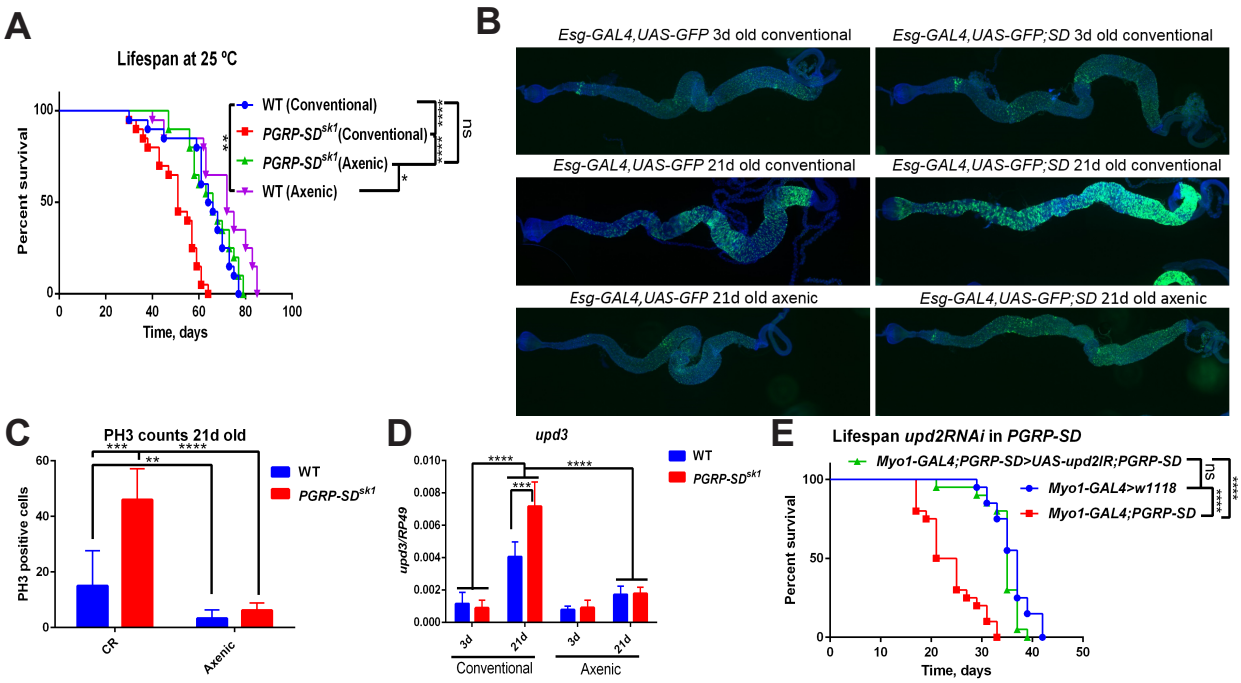
A
Lifespan at 25 ºC
Percent survival
Time, days
WT (Conventional)
PGRP-SD^sk1 (Conventional)
PGRP-SD^sk1 (Axenic)
WT (Axenic)
ns
B
Esg-GAL4,UAS-GFP 3d old conventional
Esg-GAL4,UAS-GFP;SD 3d old conventional
Esg-GAL4,UAS-GFP 21d old conventional
Esg-GAL4,UAS-GFP;SD 21d old conventional
Esg-GAL4,UAS-GFP 21d old axenic
Esg-GAL4,UAS-GFP;SD 21d old axenic
C
PH3 counts 21d old
PH3 positive cells
WT
PGRP-SD^sk1
CR
Axenic
D
upd3
upd3/RP49
WT
PGRP-SD^sk1
3d
21d
Conventional
Axenic
E
Lifespan upd2RNAi in PGRP-SD
Myo1-GAL4;PGRP-SD>UAS-upd2IR;PGRP-SD
Myo1-GAL4>w1118
Myo1-GAL4;PGRP-SD
Percent survival
Time, days
ns

Figure 3

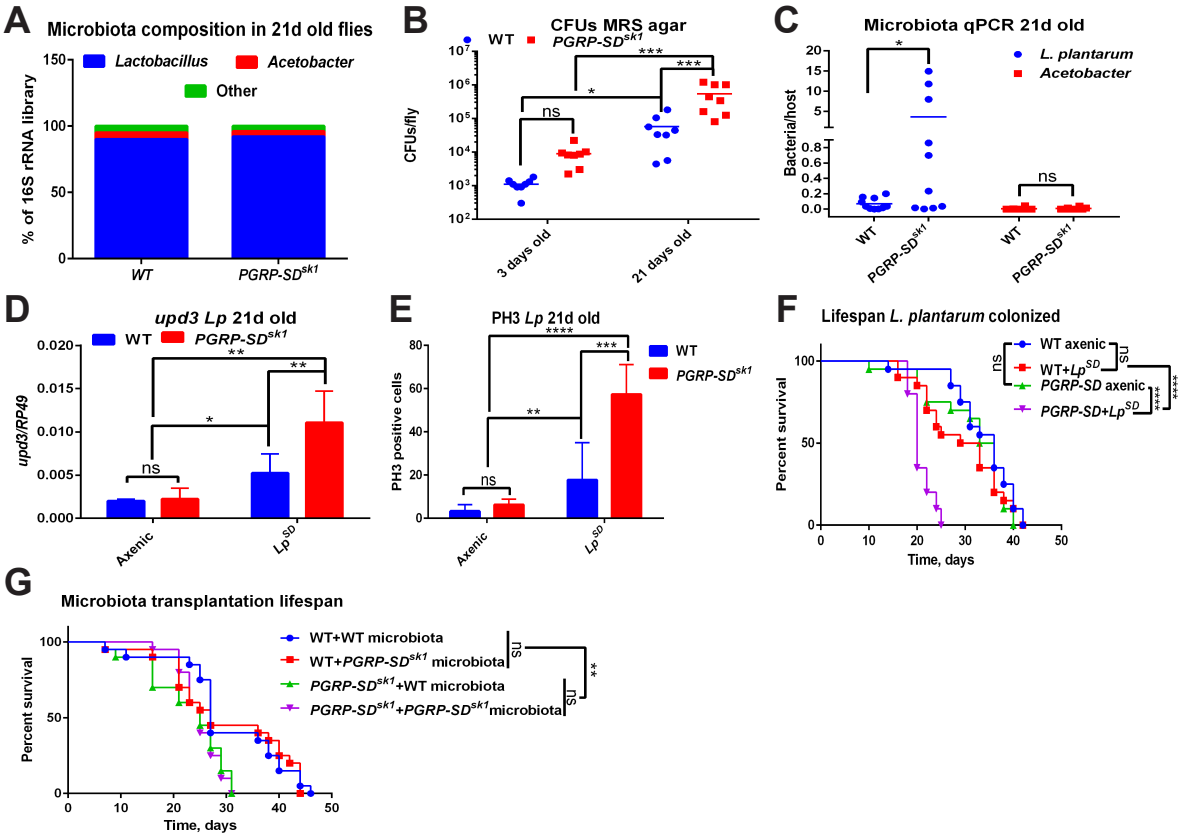
A
Microbiota composition in 21d old flies
Lactobacillus
Acetobacter
Other
% of 16S rRNA library
WT
PGRP-SD^sk1
B
CFUs MRS agar
WT
PGRP-SD^sk1
CFUs/fly
ns
3 days old
21 days old
C
Microbiota qPCR 21d old
L. plantarum
Acetobacter
Bacteria/host
ns
D
upd3 Lp 21d old
upd3/RP49
Axenic
Lp^SD
E
PH3 Lp 21d old
PH3 positive cells
F
Lifespan L. plantarum colonized
WT axenic
WT+Lp^SD
PGRP-SD axenic
PGRP-SD+Lp^SD
Percent survival
Time, days
G
Microbiota transplantation lifespan
WT+WT microbiota
WT+PGRP-SD^sk1 microbiota
PGRP-SD^sk1+WT microbiota
PGRP-SD^sk1+PGRP-SD^sk1microbiota
Percent survival
Time, days

Figure 4

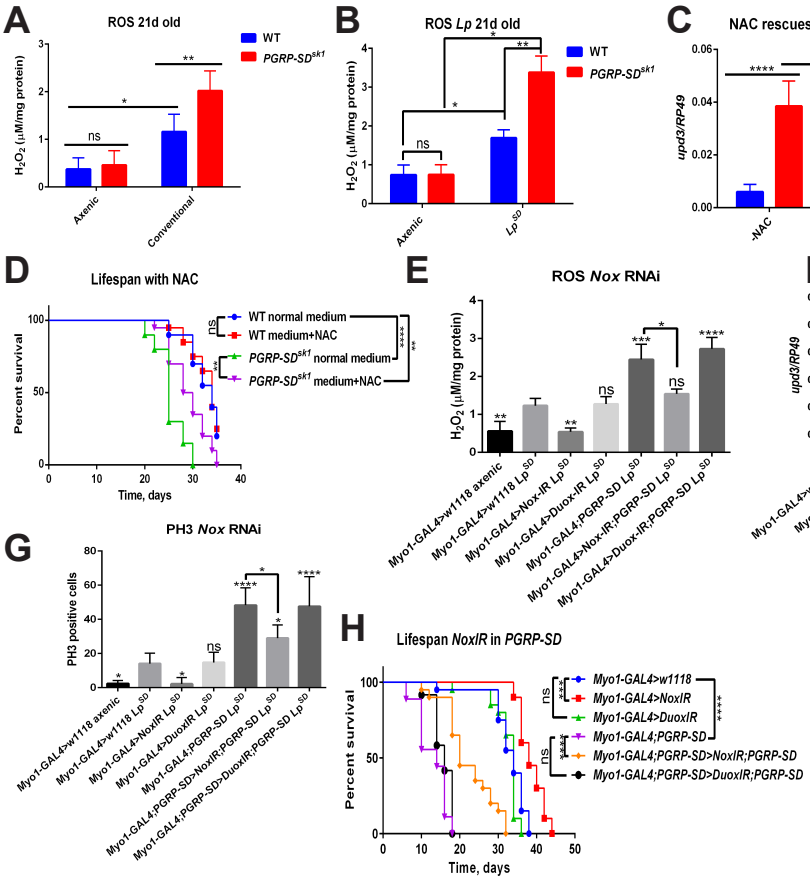
A
ROS 21d old
WT
PGRP-SD^sk1
H2O2 (µM/mg protein)
Axenic
Conventional
B
ROS Lp 21d old
Axenic
Lp^SD
C
NAC rescues upd3 in 21d old
upd3/RP49
-NAC
+NAC
D
Lifespan with NAC
Percent survival
Time, days
WT normal medium
WT medium+NAC
PGRP-SD^sk1 normal medium
PGRP-SD^sk1 medium+NAC
E
ROS Nox RNAi
Myo1-GAL4>w1118 axenic
Myo1-GAL4>w1118 Lp^SD
Myo1-GAL4>Nox-IR Lp^SD
Myo1-GAL4>Duox-IR Lp^SD
Myo1-GAL4;PGRP-SD Lp^SD
Myo1-GAL4>Nox-IR;PGRP-SD Lp^SD
Myo1-GAL4>Duox-IR;PGRP-SD Lp^SD
F
upd3 Nox RNAi
Myo1-GAL4>NoxIR Lp^SD
Myo1-GAL4>DuoxIR Lp^SD
Myo1-GAL4;PGRP-SD Lp^SD
Myo1-GAL4;PGRP-SD>NoxIR;PGRP-SD Lp^SD
Myo1-GAL4;PGRP-SD>DuoxIR;PGRP-SD Lp^SD
G
PH3 Nox RNAi
PH3 positive cells
H
Lifespan NoxIR in PGRP-SD
Myo1-GAL4>w1118
Myo1-GAL4>NoxIR
Myo1-GAL4>DuoxIR
Myo1-GAL4;PGRP-SD
Myo1-GAL4;PGRP-SD>NoxIR;PGRP-SD
Myo1-GAL4;PGRP-SD>DuoxIR;PGRP-SD

Figure 5

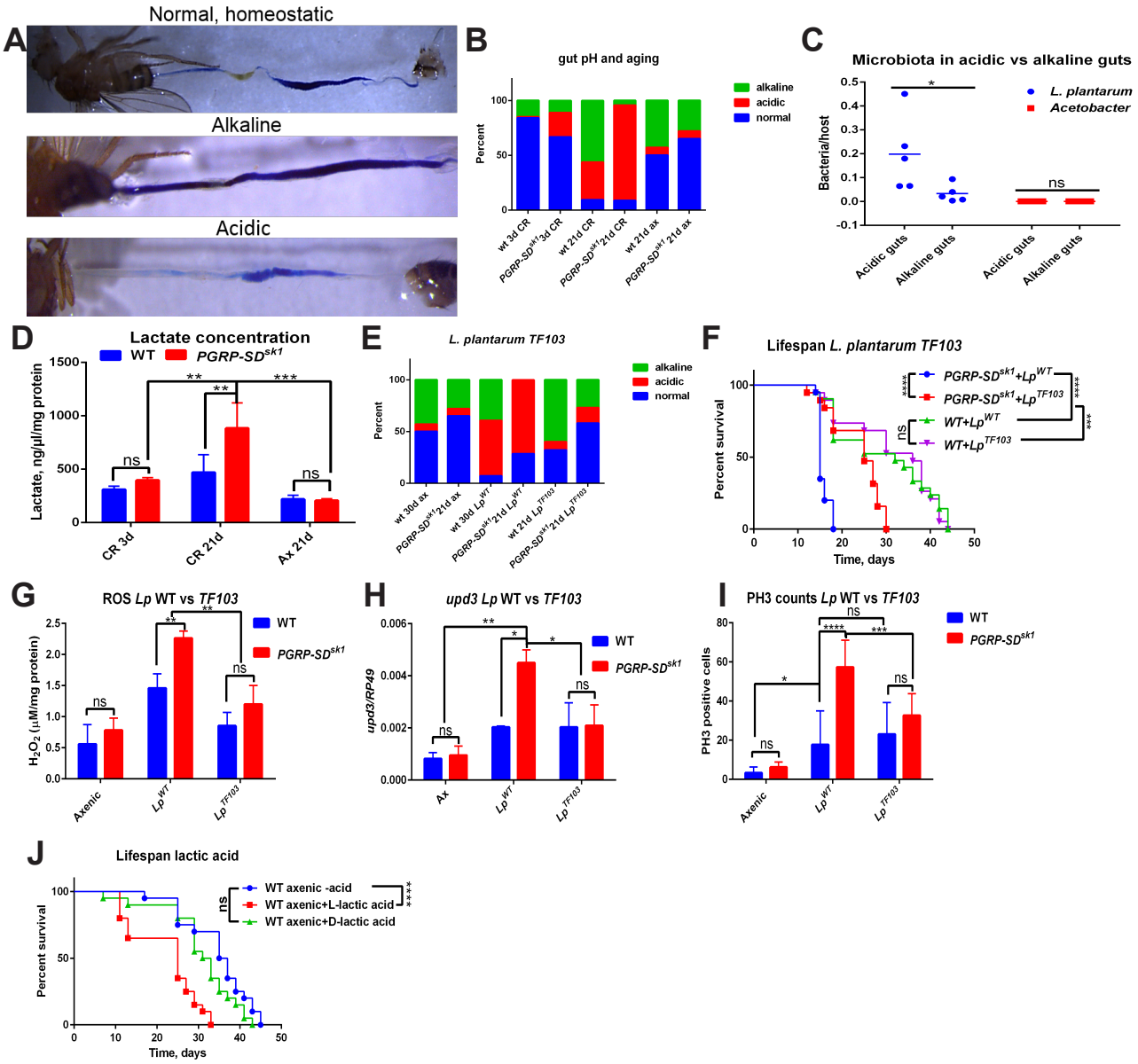
A
Normal, homeostatic
Alkaline
Acidic
B
gut pH and aging
alkaline
acidic
normal
Percent
wt 3d CR
PGRP-SD^sk1 3d CR
wt 21d CR
PGRP-SD^sk1 21d CR
wt 21d ax
PGRP-SD^sk1 21d ax
C
Microbiota in acidic vs alkaline guts
L. plantarum
Acetobacter
Bacteria/host
ns
Acidic guts
Alkaline guts
D
Lactate concentration
WT
PGRP-SD^sk1
Lactate, ng/µl/mg protein
CR 3d
CR 21d
Ax 21d
E
L. plantarum TF103
F
Lifespan L. plantarum TF103
PGRP-SD^sk1+Lp^WT
PGRP-SD^sk1+Lp^TF103
WT+Lp^WT
WT+Lp^TF103
Percent survival
Time, days
G
ROS Lp WT vs TF103
H2O2 (µM/mg protein)
Axenic
Lp^WT
Lp^TF103
H
upd3 Lp WT vs TF103
upd3/RP49
Ax
I
PH3 counts Lp WT vs TF103
PH3 positive cells
J
Lifespan lactic acid
WT axenic -acid
WT axenic+L-lactic acid
WT axenic+D-lactic acid

Figure 6

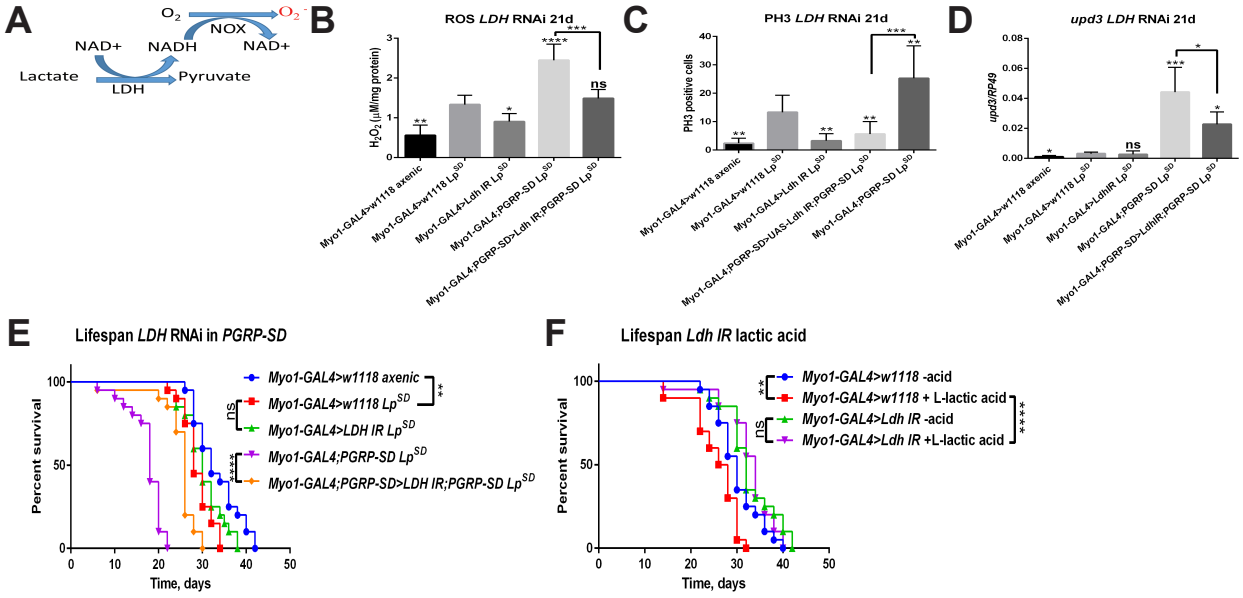
A
O2
O2-
NOX
NAD+
NADH
NAD+
Lactate
LDH
Pyruvate
B
ROS LDH RNAi 21d
H2O2 (µM/mg protein)
Myo1-GAL4>w1118 axenic
Myo1-GAL4>w1118 LpSD
Myo1-GAL4>Ldh IR LpSD
Myo1-GAL4;PGRP-SD LpSD
Myo1-GAL4;PGRP-SD>Ldh IR;PGRP-SD LpSD
C
PH3 LDH RNAi 21d
PH3 positive cells
Myo1-GAL4>w1118 axenic
Myo1-GAL4>w1118 LpSD
Myo1-GAL4>Ldh IR LpSD
Myo1-GAL4;PGRP-SD>UAS-Ldh IR;PGRP-SD LpSD
Myo1-GAL4;PGRP-SD LpSD
D
upd3 LDH RNAi 21d
upd3/RP49
Myo1-GAL4>w1118 axenic
Myo1-GAL4>w1118 LpSD
Myo1-GAL4>LdhIR LpSD
Myo1-GAL4;PGRP-SD LpSD
Myo1-GAL4;PGRP-SD>LdhIR;PGRP-SD LpSD

E
Lifespan LDH RNAi in PGRP-SD
Percent survival
Time, days
Myo1-GAL4>w1118 axenic
Myo1-GAL4>w1118 LpSD
Myo1-GAL4>LDH IR LpSD
Myo1-GAL4;PGRP-SD LpSD
Myo1-GAL4;PGRP-SD>LDH IR;PGRP-SD LpSD

F
Lifespan Ldh IR lactic acid
Percent survival
Time, days
Myo1-GAL4>w1118 -acid
Myo1-GAL4>w1118 + L-lactic acid
Myo1-GAL4>Ldh IR -acid
Myo1-GAL4>Ldh IR +L-lactic acid

Figure 7

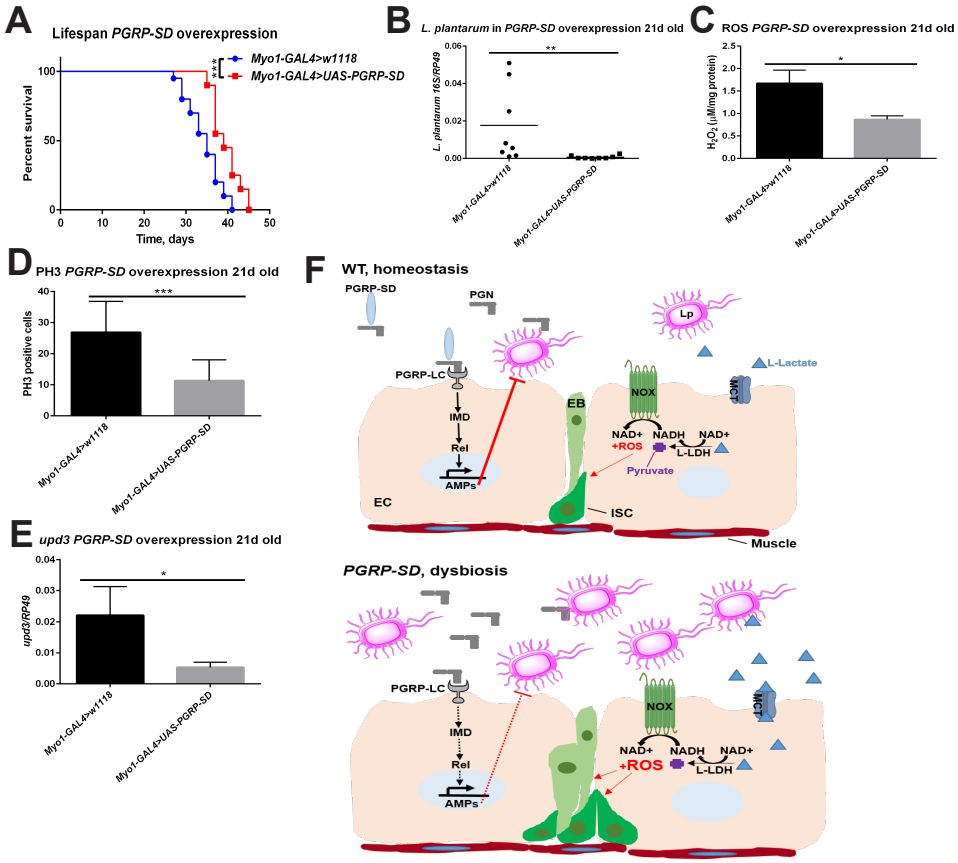
A
Lifespan PGRP-SD overexpression
Myo1-GAL4>w1118
Myo1-GAL4>UAS-PGRP-SD
Percent survival
Time, days
***
B
L. plantarum in PGRP-SD overexpression 21d old
L. plantarum 16S/RP49
**
Myo1-GAL4>w1118
Myo1-GAL4>UAS-PGRP-SD
C
ROS PGRP-SD overexpression 21d old
H2O2 (uM/mg protein)
*
Myo1-GAL4>w1118
Myo1-GAL4>UAS-PGRP-SD
D
PH3 PGRP-SD overexpression 21d old
PH3 positive cells
***
Myo1-GAL4>w1118
Myo1-GAL4>UAS-PGRP-SD
E
upd3 PGRP-SD overexpression 21d old
upd3/RP49
*
Myo1-GAL4>w1118
Myo1-GAL4>UAS-PGRP-SD
F
WT, homeostasis
PGRP-SD
PGN
Lp
L-Lactate
PGRP-LC
IMD
Rel
AMPs
EB
NOX
MCT
NAD+
+ROS
NADH
NAD+
L-LDH
Pyruvate
EC
ISC
Muscle
PGRP-SD, dysbiosis
PGRP-LC
IMD
Rel
AMPs
NOX
MCT
NAD+
+ROS
NADH
NAD+
L-LDH